

4847

**GROUNDWATER MODEL IMPROVEMENT
SUMMARY LETTER REPORT -
GEOSTATISTICAL ANALYSIS OF THE GREAT
MIAMI AQUIFER WATER LEVELS AND
URANIUM CONCENTRATIONS**

10/26/93

**DOE-FN/EPA
75⁴⁹
REPORT**

**GROUNDWATER MODEL
IMPROVEMENT SUMMARY LETTER
REPORT - GEOSTATISTICAL ANALYSIS OF
THE GREAT MIAMI AQUIFER WATER LEVELS
AND URANIUM CONCENTRATIONS**

**Fernald Environmental Management Project
October 1993**



**Submitted by:
U. S. Department of Energy
Fernald Office
P.O. Box 398705
Cincinnati, Ohio 45239-8705**

**Prepared By:
PARSONS
Fairfield, Ohio**

**Prepared For:
Fernald Environmental Restoration
Management Corporation**

**Groundwater Model Improvement
Summary Letter Report
Geostatistical Analysis of the
Great Miami Aquifer Water Levels
and Uranium Concentrations**

CONTENTS

SECTION

1.0	Introduction	1
1.1	Geostatistical Kriging Approach	1
2.0	Analysis of GMA Water Levels	5
2.1	Joint Spatial-Temporal Analysis	5
2.2	Steady-State Analysis	6
3.0	Analysis of GMA Uranium Concentrations	7
3.1	1990 Uranium Concentrations	7
3.2	1991 Uranium Concentrations	8
3.3	1992 Uranium Concentrations	9
4.0	References	10

LIST OF ILLUSTRATIONS

FIGURES

- 1 Spatial Semivariograms for 2000 Series Joint Spatial-Temporal Analysis
- 2 Temporal Semivariogram for 2000 Series Joint Spatial Temporal Analysis
- 3 Monthly 2000 Series Water Level Changes at Six Representative Locations
- 4 Estimated April, 1991 Water Levels (feet) in 2000 Series Wells
- 5 Statistical Uncertainty (feet) Associated with Water Level Estimates in Figure 4
- 6 Horizontal Semivariograms for Steady-State Analysis
- 7 Vertical Semivariogram for Steady-State Analysis
- 8 June, 1993 Head Difference Versus Vertical Separation for Spatially Clustered Wells
- 9 Estimated Steady-State Water Levels (feet) at 2000 Series Well Level
- 10 Estimated Steady-State Water Levels (feet) at 3000 Series Well Level
- 11 Estimated Steady-State Water Levels (feet) at 4000 Series Well Level
- 12 Statistical Uncertainty (feet) Associated With Steady-State 2000 Series Well Level
- 13 Statistical Uncertainty (feet) Associated With Steady-State 3000 Series Well Level
- 14 Statistical Uncertainty (feet) Associated With Steady-State 4000 Series Well Level
- 15 Horizontal Semivariograms for Log-Transformed 1990 Average Uranium Concentrations
- 16 Vertical Semivariogram for Log-Transformed 1990 Average Uranium Concentrations
- 17 Estimated 1990 Uranium Concentrations ($\mu\text{g/L}$) at 2000 Series Well Level
- 18 Estimated 1990 Uranium Concentrations ($\mu\text{g/L}$) at 3000 Series Well Level
- 19 Northeast-Southwest Vertical Cross-Section of 1990 Uranium Concentrations ($\mu\text{g/L}$)
- 20 Multiplicative Statistical Uncertainty Factor Associated With 1990 Uranium Concentration Estimates in 2000 Series Well Levels
- 21 Multiplicative Statistical Uncertainty Factor Associated With 1990 Uranium Concentration Estimates in 3000 Series Well Levels
- 22 Horizontal Semivariograms for Log-Transformed 1991 Average Uranium Concentrations
- 23 Vertical Semivariogram for Log-Transformed 1991 Average Uranium Concentrations
- 24 Estimated 1991 Uranium Concentrations ($\mu\text{g/L}$) at 2000 Series Well Level
- 25 Estimated 1991 Uranium Concentrations ($\mu\text{g/L}$) at 3000 Series Well Level
- 26 Multiplicative Statistical Uncertainty Factor Associated With 1991 Uranium Concentration Estimates in 2000 Series Well Levels
- 27 Multiplicative Statistical Uncertainty Factor Associated With 1991 Uranium Concentration Estimates in 3000 Series Well Levels
- 28 Horizontal Semivariograms for Log-Transformed 1992 Average Uranium Concentrations
- 29 Vertical Semivariogram for Log-Transformed 1992 Average Uranium Concentrations
- 30 Estimated 1992 Uranium Concentrations ($\mu\text{g/L}$) at 2000 Series Well Level
- 31 Estimated 1992 Uranium Concentrations ($\mu\text{g/L}$) at 3000 Series Well Level

LIST OF ILLUSTRATIONS (Continued)

- 32 Multiplicative Statistical Uncertainty Factor Associated With 1992 Uranium Concentration Estimates in 2000 Series Well Levels
- 33 Multiplicative Statistical Uncertainty Factor Associated With 1992 Uranium Concentration Estimates in 3000 Series Well Levels

TABLES

- 1 Summary of Analyzed Data Sets
- 2 Fitted Semivariogram Models of Spatial and Temporal Correlation

LIST OF ACRONYMS AND ABBREVIATIONS

GMA	Great Miami Aquifer
SWIFT	Sandia Waste Isolation Flow and Transport

1.0 Introduction

Geostatistical analysis provides a comprehensive method to interpolate between and extrapolate beyond spatially and temporally varying data sets and to obtain a spatially varying uncertainty value for these data sets. Geostatistical analysis of water level and uranium concentration data in the Great Miami Aquifer in the Vicinity of the FEMP has been conducted. The analysis correlates the spatial and temporal distribution of water level and uranium concentration data and defines the uncertainties associated with the analysis. These analyzed data sets will be used to help define calibration criteria for steady state flow and solute transport model calibrations.

The geostatistical analysis is part of the Model Uncertainty Analysis Task of the Model Improvement Program (see the Groundwater Modeling Evaluation Report and Improvement Plan, (DOE 1993). The approach to conducting the geostatistical analysis and the results are described in the following sections.

1.1 Background and Approach to Kriging Analysis

Kriging is a statistical interpolation method for analyzing spatially and temporally varying data. It is used to estimate parameters, like hydraulic head, on a dense grid of spatial and temporal locations covering the region of interest. At each location, two values are calculated with the kriging procedure: the estimate of the parameter of interest, and the precision of the estimate. The precision can be interpreted as the half-width of a 95 percent confidence interval for the value of the estimated parameter.

The kriging approach includes two primary analysis steps:

- 1) Estimate and model temporal and spatial correlations in the available monitoring data using a semivariogram analysis.
- 2) Use the resulting semivariogram model and the available monitoring data to estimate values at unsampled times and locations; calculate the statistical precision associated with each estimated value.

Background on the analysis methods and the specific approach used in this study are discussed in the following sections.

1.1.1 Spatial Correlation Analysis

The objective of the spatial correlation analysis is to statistically determine the extent to which measurements taken at different locations and/or times are dependent. This section is written in terms of hydraulic head measurements; however, the analysis approach is similar for any measured parameter of interest. Generally, the degree to which head measurements taken at two locations are dependent is a function of the distance between the two sampling locations. Also, for the same separation distance between two sampling locations, the spatial correlation may vary as a function of the direction between the sampling locations. For example, head values measured at each of two locations, a certain distance apart, are often more similar when the locations are at the same depth, than when they are at the same distance apart but at very different depths.

Spatial/temporal correlation is statistically assessed with the semivariogram function, $\gamma(\underline{h})$, which is defined as follows (Journel and Huijbregts 1981):

$$2\gamma(\underline{h}) = E \{ [Z(\underline{x}) - Z(\underline{x} + \underline{h})]^2 \}$$

where $Z(\underline{x})$ is the hydraulic head measured at location \underline{x} , \underline{h} is the vector of separation between locations \underline{x} and $\underline{x} + \underline{h}$, and E represents the expected value or average over the region of interest. Note that the location \underline{x} might be defined by an easting, northing, and depth coordinate, or for joint spatial/temporal data by an easting, northing, and time coordinate. Similarly, the vector of separation might be defined as a three-dimensional shift in space, or for joint spatial/temporal data as a shift in both space and time. The semivariogram is a measure of spatial dependence so that small semivariogram values correspond to high spatial correlation and large semivariogram values correspond to low correlation.

As an initial hypothesis, it is assumed that the strength of spatial correlation is a function of both distance and direction between the sampling locations. When the spatial correlation is found to depend on both separation distance and direction it is said to be anisotropic. In contrast, when the spatial correlation is the same in all directions, and therefore depends only on separation distance, it is said to be isotropic.

The spatial correlation analysis is conducted in the following steps using all available measured head data:

- 1) Experimental semivariogram curves are generated by organizing all pairs of data locations into various separation distance and direction classes (e.g., all pairs separated by 500-1,500 feet in the east-west direction ± 22.5 degrees), and then calculating within each class the average squared-difference between the measurements taken at each pair of locations. The results of these calculations are plotted against separation distance and by separation direction.
- 2) A variety of experimental semivariogram curves are generated by separating the data into discrete zones, such as different depth horizons or time periods. If significant differences are found in the semivariograms they are modeled separately; if not, the data are pooled together into a single semivariogram.
- 3) After the data have been pooled or separated accordingly, and the associated experimental semivariograms have been calculated and plotted, a positive-definite analytical model is fitted to the experimental curve(s). The fitted semivariogram model is then used as the spatial correlation structure for the subsequent kriging interpolation.

In this study, the computer software used to perform the geostatistical calculations was the GSLIB software written by the Department of Applied Earth Sciences at Stanford University, and documented and released by Prof. Andre Journel and Dr. Clayton Deutsch (Deutsch and Journel 1992). Some computational details concerning the calculation of semivariograms are as follows:

- 1) The primary subroutine used to calculate experimental semivariograms was GAMV3, which is used for three-dimensional, irregularly spaced data.
- 2) For three-dimensional spatial analyses, horizontal separation distance classes were defined in increments of 1000 feet with a tolerance of 500 feet, while vertical distances were defined in increments of 20 feet with a tolerance of 10 feet. Horizontal separation directions were defined in the four primary directions of north, northeast, east, and southeast with a tolerance of 22.5 degrees.
- 4) For the joint spatial/temporal analysis, spatial separation distances and directions were defined in the same way as described immediately above, although there was no vertical direction associated with this analysis. For the temporal portion of this analysis, separation distance classes were defined in increments of 30 days with a tolerance of 15 days.

1.1.2 Interpolation Using Ordinary Kriging

Ordinary kriging is a linear geostatistical estimation method which uses the semivariogram function to determine the estimated head values and the precision associated with the estimates (Journel and Huijbregts 1981). Kriging is different from other classical interpolation and contouring algorithms. in that it produces statistically optimal estimates and associated precision measures.

The kriging analysis was conducted in this study using the GSLIB computer software (subroutine KTB3D). The primary steps involved in this analysis were as follows:

- 1) A three-dimensional grid was defined, specifying the locations at which estimated head values are required. The horizontal origin of this grid (southernmost point) was at Ohio State Planar Coordinates 469,197.58 feet north and 1,379,948.62 feet east. The network included 112 blocks in the northern direction (rotated 30 degrees west of North) and 120 blocks in the eastern direction. All blocks were 125 feet square. For three-dimensional spatial kriging, the vertical origin was at 390 feet above sea level, and the network included 30 vertical blocks each 5 feet thick. For joint spatial/temporal kriging, the network included 43 monthly blocks in increments of 30 days, starting at January 20, 1990.

This grid was set to match the latest Sandia Waste Isolation Flow and Transport (SWIFT) groundwater flow and transport model grid in the XY dimension in order to facilitate the defining of model boundary conditions and model calibration criteria. Vertical discretization of the kriging output could not match the SWIFT layering because the SWIFT model layers were being revised concurrent with the geostatistical analysis. However, the resulting vertical discretization can be easily translated to the model layers.

- 2) At each block in the grid, the average hydraulic head across the block was estimated using all measured data found within a pre-defined search radius. For three-dimensional spatial kriging, the search radius was 6,000 feet in all directions. For joint spatial/temporal kriging, the search radius was 6,000 feet in space and 72 days in time.
- 3) After the available data were identified for each grid block, the appropriate data weighting, estimated head value, and estimation precision were calculated using the appropriate semivariogram model.
- 4) Output from the kriging process was post processed using a Fortran routine to create vertical values of head (or concentration) at the centroid of each model block. Since SWIFT model layers 1, 3, and 6 correlate to 2000, 3000, and 4000 monitoring depths, these kriged values provide estimates of head (or concentration) at model grid centroids that correspond to the monitoring depths.

- 5) Output from the kriging process was typically displayed in the form of contour maps, to represent spatial variations, and time-series graphs to represent temporal variations.

2.0 Analysis of GMA Water Levels

Steady-state water levels in the Great Miami Aquifer (GMA) are needed for calibration of the steady-state groundwater flow model. A two-step data analysis approach was used to estimate the steady-state water levels.

- 1) A joint spatial-temporal kriging analysis was performed to estimate monthly water level changes in 2000 series wells and to select a single month that is representative of steady-state conditions.
- 2) A three-dimensional spatial kriging analysis was performed with data from the selected month in the 2000, 3000, and 4000 series wells to estimate steady-state hydraulic heads.

2.1 Joint Spatial-Temporal Analysis

The joint spatial-temporal kriging analysis was performed using monthly water level measurements collected during the period from January, 1990 through July, 1993 in one hundred, seventy-seven 2000 series wells. As shown in Table 1, there were a total of 3,791 such measurements. The semivariogram curves, quantifying spatial and temporal correlation in these data, are shown in Figures 1 and 2. The spatial semivariograms in Figure 1 were calculated for four standard directions (relative to the groundwater model grid system) denoted 0 degrees (north), 45 degrees (northeast), 90 degrees (east), and 135 degrees (southeast). These semivariograms show clear anisotropy with the highest variabilities directed north 180 degrees to the predominant flow direction, and the lowest variabilities directed east perpendicular to the predominant flow direction. The corresponding temporal semivariogram for the 2000 series monthly water levels is shown in Figure 2. Note that the units for separation distances between data locations are in days in Figure 2 and in feet in Figure 1. The semivariograms in Figures 1 and 2 were modeled with an anisotropic mathematical model containing three nested variance structures. The parameters of the model are listed in Table 2. Note in this table that three types of semivariogram models were used in various parts of these analyses: spherical, gaussian, and linear models. These models are fully described by Journel and Huijbregts (1981).

The monthly 2000 series water levels were used along with the semivariogram model to estimate monthly changes in water levels across the entire groundwater modeling grid. The time period for this kriging analysis was taken as every 30 days starting January 20, 1990 and ending July 2, 1993. The monthly water levels (in feet above mean sea level) are depicted in Figure 3 for six locations

uniformly spaced across the groundwater modeling grid. This figure shows that water levels during this period were relatively high in 1990, decreased in 1991, were relatively low in 1992, and are increasing in 1993. Spatial variability across the grid is depicted in Figure 4 for April, 1991 water levels (in feet). As expected, this figure shows a general trend of decreasing hydraulic heads to the south associated with the predominant flow direction south and to the east to the Great Miami River. Figure 5 presents the statistical uncertainty (in feet) associated with the water level estimates in Figure 4. These uncertainties can be interpreted as half-widths of a 95 percent confidence interval for the estimates. That is, the confidence interval for the April 1991 water level at any location in the grid is

$$\text{HEAD} \pm \text{PREC}$$

where HEAD is the estimated water level from Figure 4 and PREC is the estimation uncertainty from Figure 5. Note in Figure 5 that in this case most of the estimation uncertainties are from 2 to 4 ft.

2.2 Three-Dimensional Spatial Analysis for Steady State Heads

The primary reason for performing the joint spatial-temporal analysis was to select for the steady-state analysis, a single month which was representative of average water levels during the 1990-1993 time period. Examining the results in Figure 3, it appears that 3 months can be considered representative: January 1990; November 1991; and June 1993 (represented as months 1, 23, and 41 in Figure 3). Water levels in each of these 3 months appear to be approximately equal to the average water level across the entire 1990-1993 time period. However, several new wells were installed in the area in 1993, particularly in the southeastern part of the modeling grid. Therefore, a significantly greater number of water level measurements were available for June 1993 in comparison with January 1990 and November 1991. As a result, June 1993 was selected as the month to represent steady-state conditions.

As shown in Table 1, water level measurements for June 1993 were available for the steady-state kriging analysis in 202 wells at the 2000, 3000, and 4000 series depths. The three-dimensional spatial semivariograms for these data are shown in Figures 6 and 7. As in the joint spatial-temporal analysis (Figure 1), horizontal semivariograms in Figure 6 were calculated in four primary directions. In addition, the semivariogram in Figure 7 was calculated in the vertical direction. Note in Figure 7 that, except for one point at a separation distance of about 75 feet, the vertical variability among the June 1993 water levels is quite low. This same result is further indicated by Figure 8 which plots water level differences as a function of vertical separation for pairs of spatially clustered wells. Note in Figure 8 that these differences are almost always less than 1 or 2 feet.

A kriging analysis was performed with the June 1993 data and the semivariogram model shown in Figures 6 and 7, as well as Table 2. This analysis estimated steady-state water levels across the groundwater modeling grid at regular 5 feet vertical intervals from 390 to 540 feet above sea level.

The horizontal variability in steady-state water levels for the 2000, 3000, and 4000 series well layers are shown in Figures 9, 10, and 11. These figures show a southerly direction of flow on the western and southern part of the grid and an easterly direction of flow (with a flat gradient) across the site toward the Great Miami River. One significant feature in these figures is the major water level depression caused by the three production wells in the eastern portion of the grid. Similar patterns are exhibited in the three well screen zones indicating strong vertical continuity of water levels and predominantly horizontal flow. Local differences in the heads between the three levels can also be noted. Figures 12, 13, and 14 which presents the statistical uncertainty associated with the estimates in Figures 9, 10, and 11 shows that the steady-state water levels are generally estimated to within 1 or 2 feet, although the southeast corner showed higher values (greater than 5 feet) due to the lack of data in this area of the grid.

3.0 Analysis of GMA Uranium Concentrations

Estimated GMA uranium levels are needed for calibration of the groundwater solute transport model. Separate three-dimensional spatial kriging analyses, similar to that for steady-state water levels, were performed using average uranium levels measured during 1990, 1991, and 1992. One important difference between these uranium analyses and the water level analysis was that a logarithmic transformation of the uranium data was performed prior to the semivariogram and kriging analyses. This transformation was required to reduce the extreme variability seen in the uranium concentrations. After the kriging step, the estimates and statistical uncertainties were back-transformed with an inverse-logarithmic transformation. As a result of this procedure, the 95 percent confidence intervals for uranium concentrations are multiplicative, rather than additive, in format. That is, the confidence interval at any location in the grid is from;

$$(\text{CONC}-\text{CONC}/\text{PREC}) \text{ to } (\text{CONC}+\text{CONC}*\text{PREC})$$

"CONC" is the back-transformed estimated uranium concentration and "PREC" is the back-transformed estimation uncertainty.

3.1 1990 Uranium Concentrations

The spatial kriging analysis was performed using average uranium concentrations ($\mu\text{g/L}$) measured during 1990 in 169 wells at the 2000, 3000, and 4000 series depths. As shown in Table 1, the mean of these measurements was $29.3 \mu\text{g/L}$, although the maximum concentration ($691 \mu\text{g/L}$) was considerably higher. The overall variability in the uranium data, as measured by the coefficient of variation, was also relatively high (2.90), particularly in comparison with that of the water level data (0.01).

Horizontal semivariograms were calculated in the four primary directions (Figure 15), and indicated no significant anisotropy; that is, all four directional curves exhibit the same shape and variability. The vertical semivariogram (Figure 16) was found to plateau at the same overall variance [$3.0 (\mu\text{g/L})^2$], as the horizontal semivariograms. However, the vertical semivariogram reaches a plateau at a separation distance of about 120 feet while the horizontal semivariograms reach a plateau at a separation distance of about 3,000 feet. As a result, a geometric anisotropic semivariogram model was fitted to these curves, as shown in Figures 15 and 16. The details of these models are summarized in Table 2.

A three-dimensional kriging analysis was performed using the 1990 average uranium concentrations and the semivariogram model discussed above. The resulting estimated spatial distribution of the uranium concentrations is depicted for the 2000 and 3000 well levels in Figures 17 and 18, respectively. The most significant uranium concentrations, those above $70 \mu\text{g/L}$, occur in a northeast oriented area extending about 2,500 feet by 900 feet horizontally, and about 40 feet vertically. A surrounding area, about five to ten times larger, contains lower uranium concentrations between 10 and $70 \mu\text{g/L}$. The uranium plume in the southern area (South Plume) is more elongated at the 2000 series level than the 3000 (as defined by the $10 \mu\text{g/L}$ contour). Based on an inspection of the output file, the maximum uranium concentration in the 4000 series level is $8.2 \mu\text{g/L}$ and the mean concentration is $1.57 \mu\text{g/L}$, thus the uranium concentrations are not contoured for the 4000 series well. A sample vertical section cut along the long axis of the plume shown in Figure 17 is shown in Figure 19. This figure shows the vertical trace of contamination covering both the 2000 and 3000 series elevations, but not extending to the 4000 level. Figures 20 and 21, which present the statistical uncertainty associated with the estimates in Figures 17 and 18, indicate the uranium concentrations are typically estimated to within a multiplicative factor of 10; that is, the true concentrations could be 10 times higher or lower.

3.2 1991 Uranium Concentrations

The 1991 uranium spatial kriging analysis was performed in the same way as that for 1990 uranium levels. As shown in Table 1, 163 average 1991 uranium concentrations were analyzed, with a mean concentration of $35.1 \mu\text{g/L}$ and a maximum concentration of $1,572.5 \mu\text{g/L}$. The broader range of 1991 uranium concentrations in comparison with 1990 levels is also reflected in the coefficients of variation (4.62 for 1991 data versus 2.90 for 1990 data).

Horizontal and vertical semivariograms were calculated with the log-transformed 1991 uranium data and are shown in Figures 22 and 23. These figures show a very similar structure to those for the 1990 uranium data (Figures 15 and 16), although the overall variance for the 1991 data [$3.8 (\mu\text{g/L})^2$] is higher than that for the 1990 data [$3.0 (\mu\text{g/L})^2$]. As a result, a similar geometric anisotropic semivariogram model was fitted for the 1991 uranium data, as shown in Figures 22 and 23, and Table 2.

A three-dimensional kriging analysis was performed with the 1991 uranium data. The resulting estimated spatial distribution of the uranium concentrations is depicted for the 2000 and 3000 levels in Figures 24 and 25, respectively. Qualitatively, the results were quite similar to those for the 1990 uranium levels. Like 1990, the most significant uranium concentrations, those above 70 $\mu\text{g/L}$, occur in a northeast oriented area about 40 feet vertically. A surrounding area, about five to ten times larger, contains lower uranium concentrations between 10 and 70 $\mu\text{g/L}$. The uranium plume in the southern area (South Plume) is similar at the 2000 series level and the 3000 (as defined by the 10 $\mu\text{g/L}$ contour), although the 10 $\mu\text{g/L}$ contour at the 2000 level extends further north. Based on an analysis of the output file, the maximum uranium concentration in the 4000 series level is 18.9 $\mu\text{g/L}$ and the mean concentration is 1.75 $\mu\text{g/L}$, thus the uranium concentrations are not contoured for the 4000 series well level. Comparing the 1991 and 1990 uranium levels (Figures 24, 25, 17, and 18) indicates that the magnitude and extent of the most significant concentrations were still approximately the same. However, because of the marginally higher variability in 1991 uranium concentrations versus those in 1990, the statistical uncertainty of the 1991 uranium estimates (Figures 26 and 27) is somewhat higher (approximately 25 percent higher) than that of the 1990 estimates (Figures 20 and 21).

3.3 1992 Uranium Concentrations

The kriging analysis for 1992 uranium concentrations was performed in a similar manner to the analyses of 1990 and 1991 uranium levels. However, the 1992 uranium data were found to be quite different. As shown in Table 1, 153 average 1992 uranium concentrations were analyzed. The 1992 mean concentration (6.7 $\mu\text{g/L}$) was found to be substantially lower than those in 1990 (29.3 $\mu\text{g/L}$) and 1991 (35.1 $\mu\text{g/L}$). Likewise, the coefficient of variation for the 1992 data (2.28) was lower than those in 1990 (2.90) and 1991 (4.62). It appears that the primary reason for these differences is that while many of the same wells were sampled for uranium in 1990 and 1991, a large number of different wells were sampled in 1992. A formal statistical analysis of these joint spatial-temporal changes in uranium concentrations has not yet been performed.

Horizontal and vertical semivariograms for the log-transformed 1992 uranium data are presented in Figures 28 and 29. In general, these figures show a similar structure to those for the 1990 and 1991 uranium data (Figures 17, 18, 24, and 25). However, the overall variance for the 1992 data is lower, although it appears that the very short scale variability (i.e., for separation distances less than 700 feet) may be larger for the 1992 data. Because of this latter possibility, two different semivariogram models were considered (see Figures 28 and 29). Kriging of the solid line model, showing larger short scale variability, resulted in excessive spatial smoothing of the estimated uranium concentrations with a tendency to "average out" and mask potential high concentration areas. In contrast, use of the dotted-line model tends to accentuate potential high concentration areas and thus provide conservative worst-case estimates. For this reason, it was decided to use the dotted-line semivariogram model in the subsequent kriging step.

A three-dimensional kriging analysis was performed with the 1992 uranium data. The resulting estimated spatial distribution of the uranium concentrations is illustrated for the 2000 and 3000 levels in Figures 30 and 31, respectively. Qualitatively, the pattern of the results are similar to those for the 1990 and 1991 uranium levels. Like 1990 and 1991, the most significant uranium concentrations occur in an area near Willey Road with a maximum value of 40 $\mu\text{g/L}$. A surrounding area, about five to ten times larger, contains lower uranium concentrations (less than 10 $\mu\text{g/L}$). The 10 $\mu\text{g/L}$ contour stretches along Paddys Run from the waste pits to south of Willey Road. The 3000 level results only show three small areas greater than 10 $\mu\text{g/L}$ (Figure 31). The 1992 results show considerably less uranium than the 1990 and 1991 results. Based on an analysis of the output file, the maximum uranium concentration in the 4000 series level is 3.6 $\mu\text{g/L}$ and the mean concentration is 0.81 $\mu\text{g/L}$, thus the uranium concentrations are not contoured for the 4000 series well level. Figures 32 and 33 show the contour plots of the statistical uncertainty. The statistical uncertainty of the 1992 uranium estimates (Figures 32 and 33) is similar to the 1991 estimates (Figures 26 and 27).

4.0 References

Deutsch, Clayton V., and Andre G. Journel, 1992, GSLIB: Geostatistical Software Library and User's Guide, Oxford University Press, New York, 340 pp.

DOE 1993, Groundwater Modeling Evaluation Report and Improvement Plan, ERA Project, FEMP. Fernald, Ohio

Journel, A.G., and Ch.J. Huijbregts, 1981, Mining Geostatistics, Academic Press, reprinted with corrections, 600 pp.

Table 1 - Summary of Analyzed Data Sets

Data Set	Number of Data	Minimum Value	Maximum Value	Mean	Standard Deviation	Coefficient of Variation
2000 Series Wells Joint Spatial-Temporal Water Levels in ft.	3791	493.7 ft.	568.9 ft.	519.9 ft.	5.3 ft.	0.01
Steady-State Water Levels in ft. (June, 1993 Data)	202	497.4 ft.	539.1 ft.	520.8 ft.	4.4 ft.	0.01
1990 Uranium Levels in $\mu\text{g/L}$	169	0.25 $\mu\text{g/L}$	691 $\mu\text{g/L}$	29.3 $\mu\text{g/L}$	85.1 $\mu\text{g/L}$	2.90
1991 Uranium Levels in $\mu\text{g/L}$	163	0.05 $\mu\text{g/L}$	1572.6 $\mu\text{g/L}$	35.1 $\mu\text{g/L}$	162.3 $\mu\text{g/L}$	4.62
1992 Uranium Levels in $\mu\text{g/L}$	153	0.08 $\mu\text{g/L}$	149.2 $\mu\text{g/L}$	6.7 $\mu\text{g/L}$	15.3 $\mu\text{g/L}$	2.28

4842

Table 2 - Fitted Semivariogram Models of Spatial and Temporal Correlation

Data Set	Semivariogram Model
2000 Series Wells Joint Spatial-Temporal Water Levels in ft.	<p>$K = 3$ Nested Structures, Nugget Variance = 0 ft.²</p> <ol style="list-style-type: none"> 1. Geometric Anisotropic Spherical, Variance = 1.5 ft.², Spatial Range = 1200 ft., Temporal Range = 30 days (represented by solid line on Figure 1) 2. Geometric Anisotropic Spherical, Variance = 5.5 ft.², Spatial Range = 7000 ft., Temporal Range = 700 days (represented by dashed line on Figure 1) 3. Zonal Gaussian in Spatial NS Direction, Variance = 22 ft.², Spatial NS Range = 6060 ft. (represented by dotted line on Figure 1)
Steady-State Water Levels in ft. (June, 1993 Data)	<p>$K = 2$ Nested Structures, Nugget Variance = 0 ft.²</p> <ol style="list-style-type: none"> 1. Isotropic Linear, Slope = 0.00045 ft.²/ft. (represented by solid line on Figure 6) 2. Zonal Gaussian in Horizontal NS Direction, Variance = 13 ft.², NS Range = 8660 ft. (represented by dashed line on Figure 6)
1990 Uranium Levels in $\mu\text{g/L}$	<p>$K = 1$ Structure, Nugget Variance = $0.3 [\ln(\mu\text{g/L})]^2$</p> <ol style="list-style-type: none"> 1. Geometric Anisotropic Spherical, Variance = $2.7 [\ln(\mu\text{g/L})]^2$, Horizontal Range = 3000 ft., Vertical Range = 120 ft.
1991 Uranium Levels in $\mu\text{g/L}$	<p>$K = 1$ Structure, Nugget Variance = $0.4 [\ln(\mu\text{g/L})]^2$</p> <ol style="list-style-type: none"> 1. Geometric Anisotropic Spherical, Variance = $3.4 [\ln(\mu\text{g/L})]^2$, Horizontal Range = 3000 ft., Vertical Range = 105 ft.
1992 Uranium Levels in $\mu\text{g/L}$	<p>$K = 1$ Structure, Nugget Variance = $0.4 [\ln(\mu\text{g/L})]^2$</p> <ol style="list-style-type: none"> 1. Geometric Anisotropic Spherical, Variance = $2.0 [\ln(\mu\text{g/L})]^2$, Horizontal Range = 3000 ft., Vertical Range = 105 ft.

2000 Wells Joint s/t - spatial

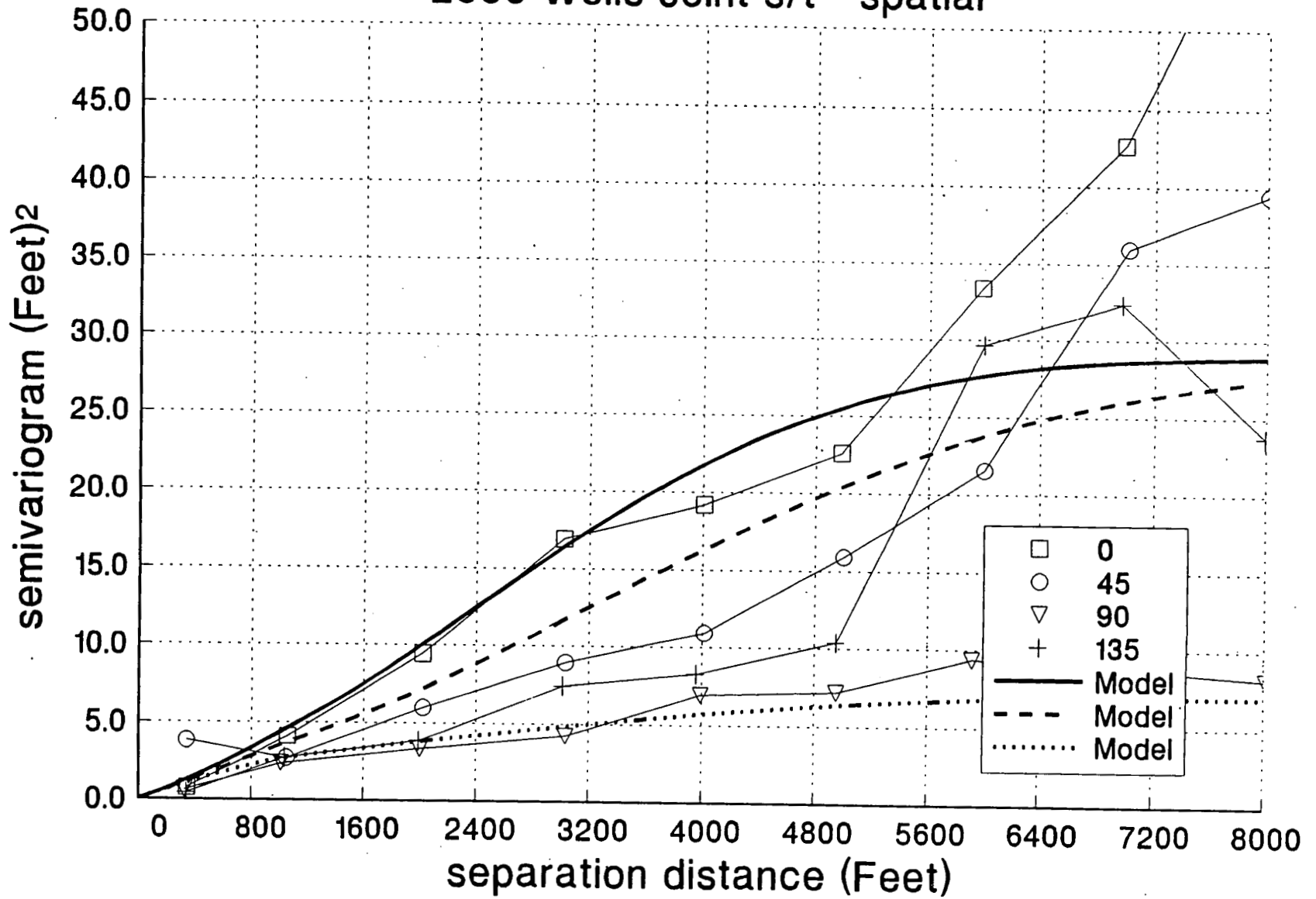


Figure 1 - Spatial Semivariograms for 2000 Series Joint Spatial-Temporal Analysis
 BRAFS11VOL1:RSAPPS\RSDATA\
 OU-SIPO-37GEOSTAT

-13-

Rev. No.: 0

4842

17A

2000 Wells Joint s/t - temporal

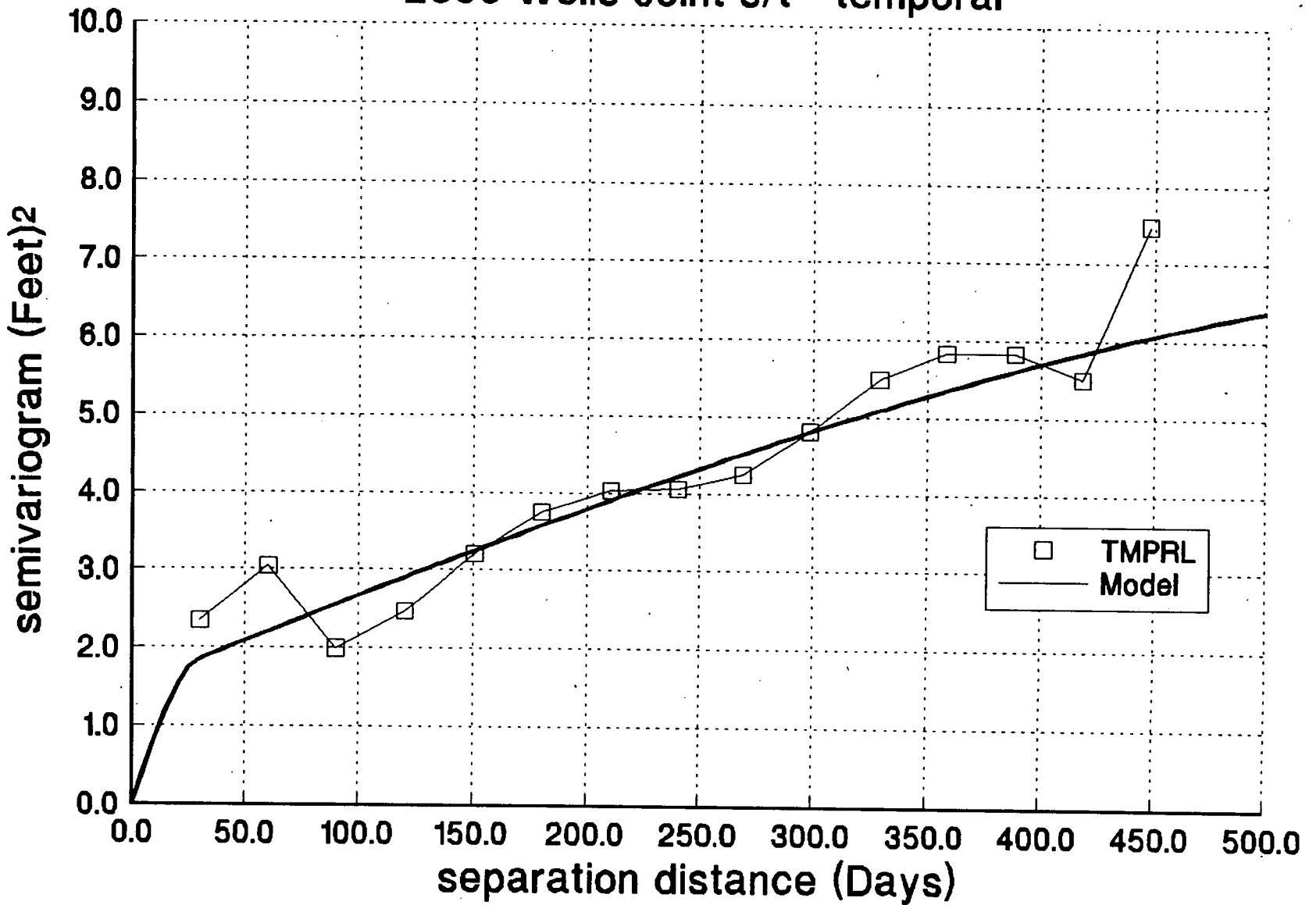


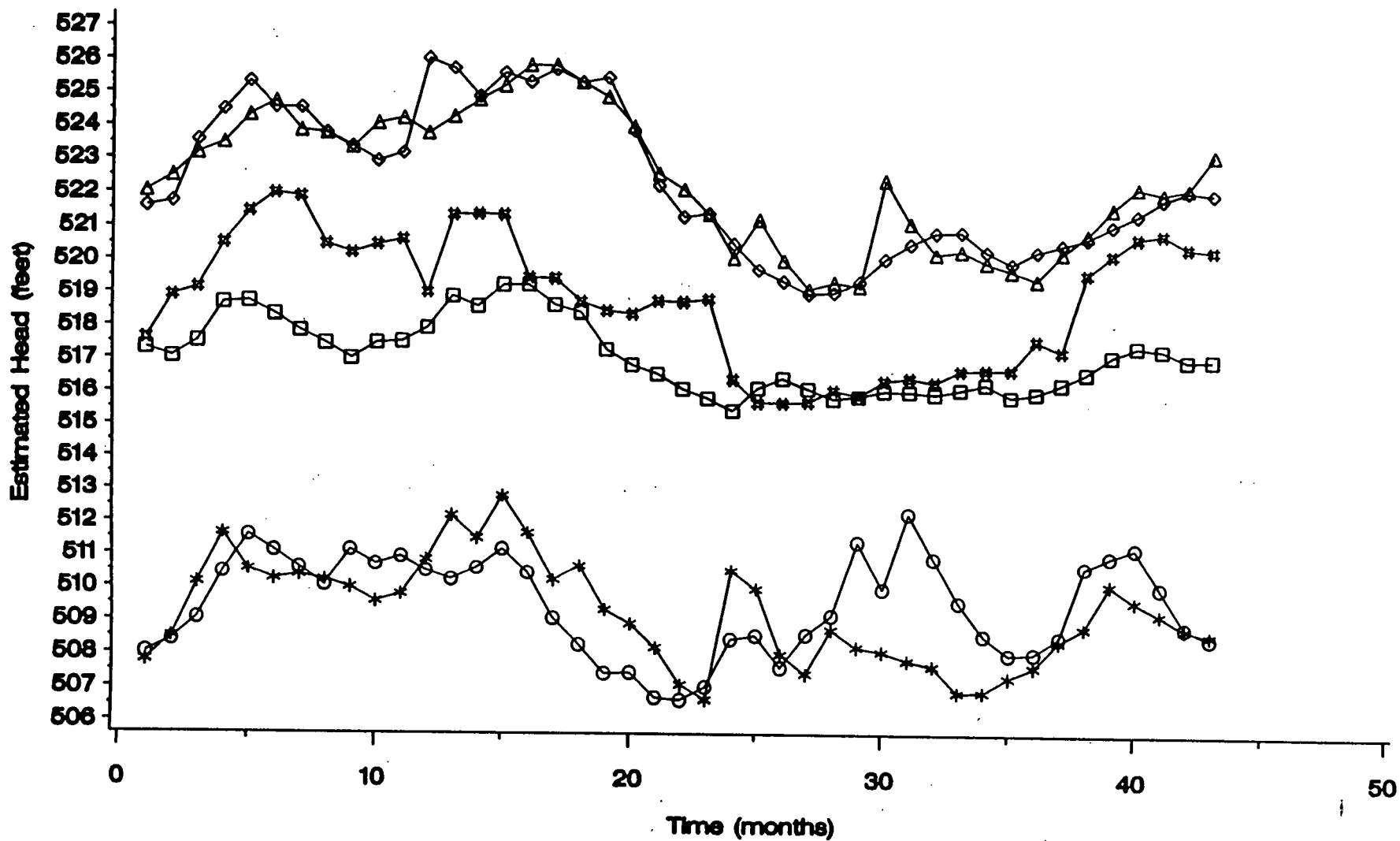
Figure 2 - Temporal Semivariogram for 2000 Series Joint Spatial Temporal Analysis
 ERAFS\I\VOL1\RSAPPS\RSDATA\
 OU-5\PO-37\GEOSTAT

-14-

Rev. No.: 0

2787

Temporal Profile of 6 Selected Estimation Locations for 1990-1993



Grid Location	*-*-* (10,10)	○-○-○ (80,10)	□-□-□ (40,30)
	--* (80,30)	△-△-△ (10,90)	◇-◇-◇ (60,90)

Figure 3 - Monthly 2000 Series Water Level Changes at Six Representative Locations
 ERAFS1VOL1:RSAPPSRSDATA\
 OU-51PO-37GEOSTAT

-15-

Rev. No.: 0

4842

4847

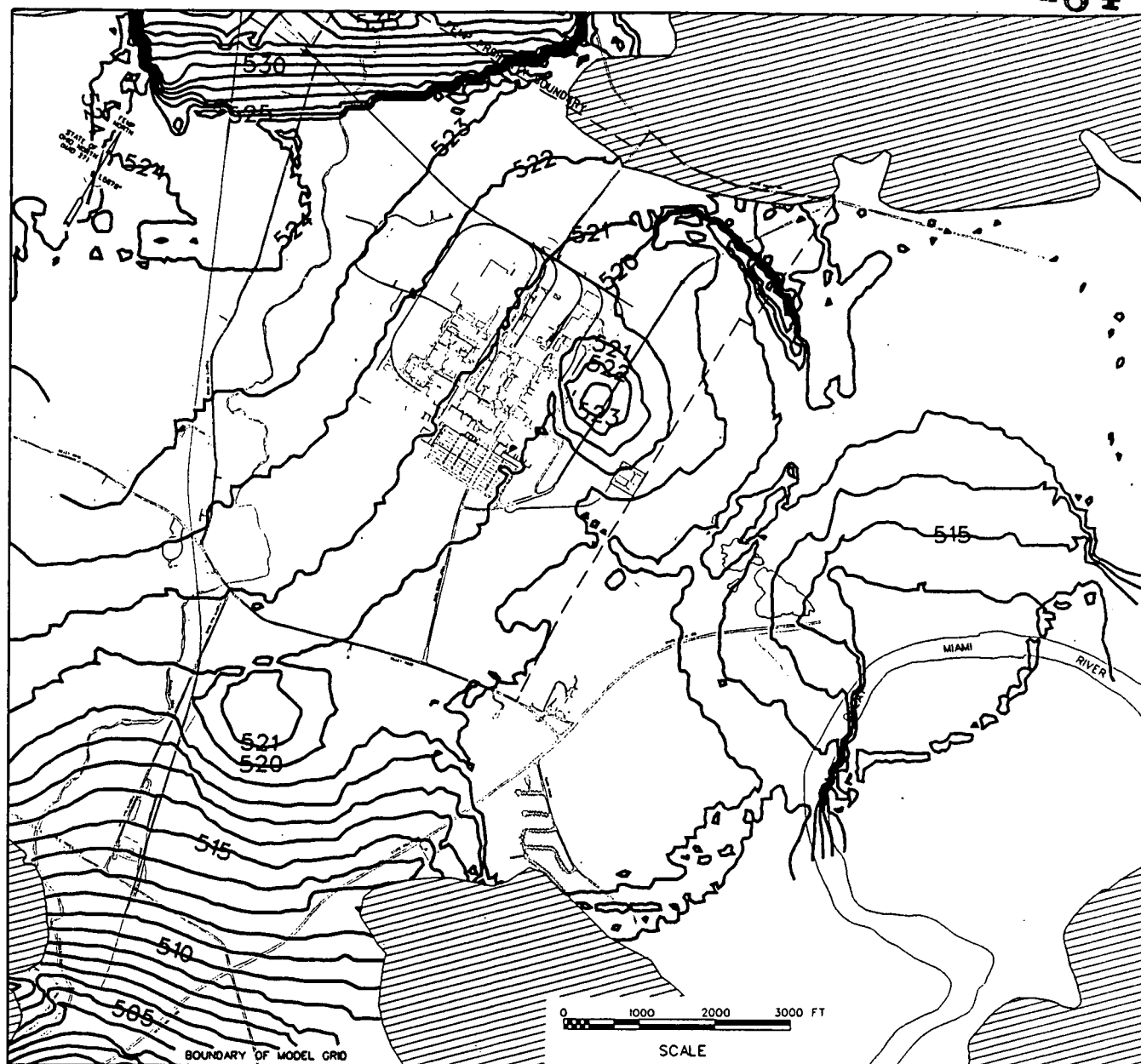


Figure 4 - Estimated April, 1991 Water Levels (feet) in 2000 Series Wells

ERAFS1\VOL1:RSAPPS\RSDATA\
OU-5\PO-37\GEOSTAT

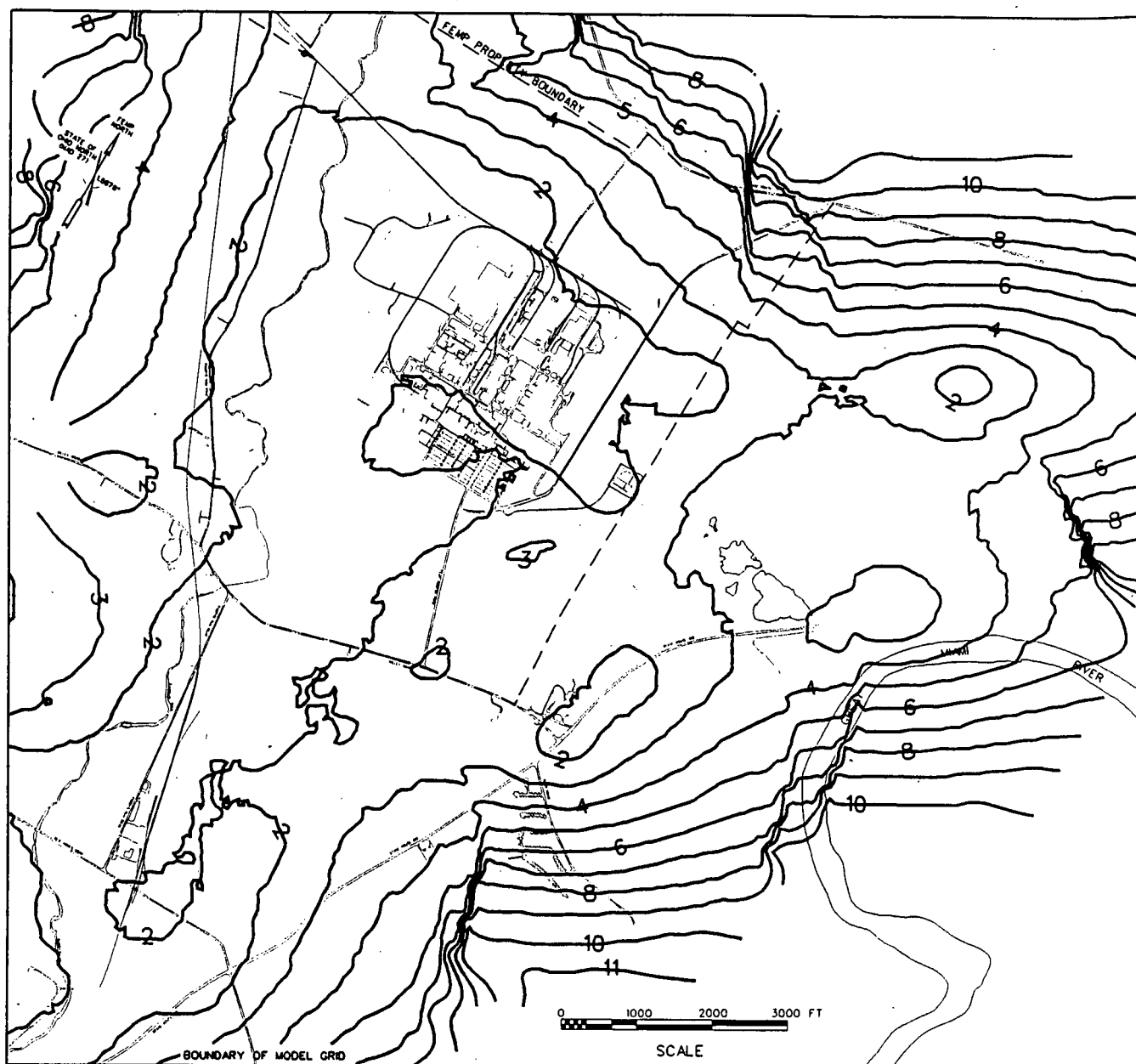


Figure 5 - Statistical Uncertainty (feet) Associated with Water Level Estimates in Figure 4
 ERAFS1\VOL1\RSAPPS\RSDATA\
 OU-5\PO-37\GEOSTAT

steady state Horizontal

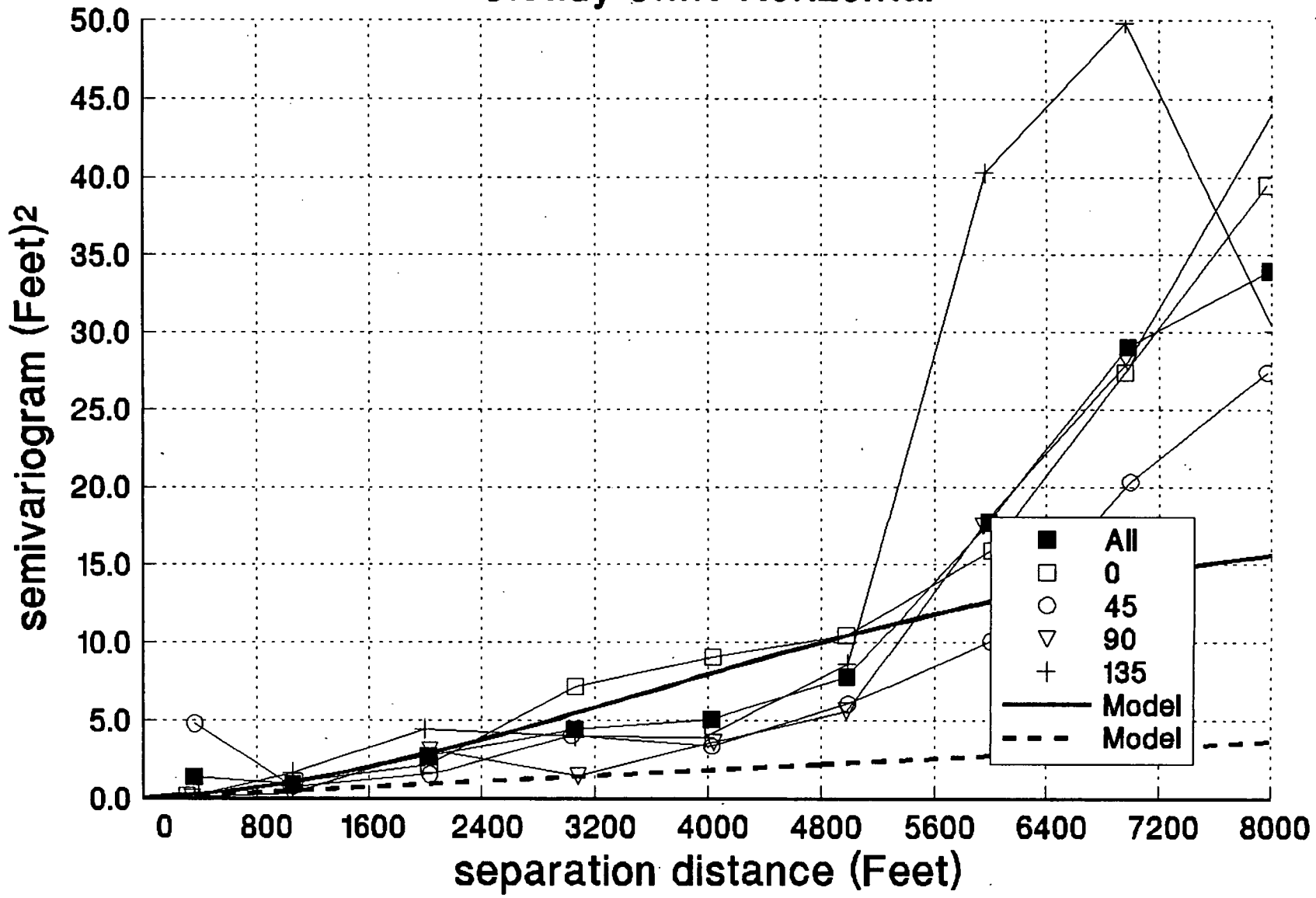
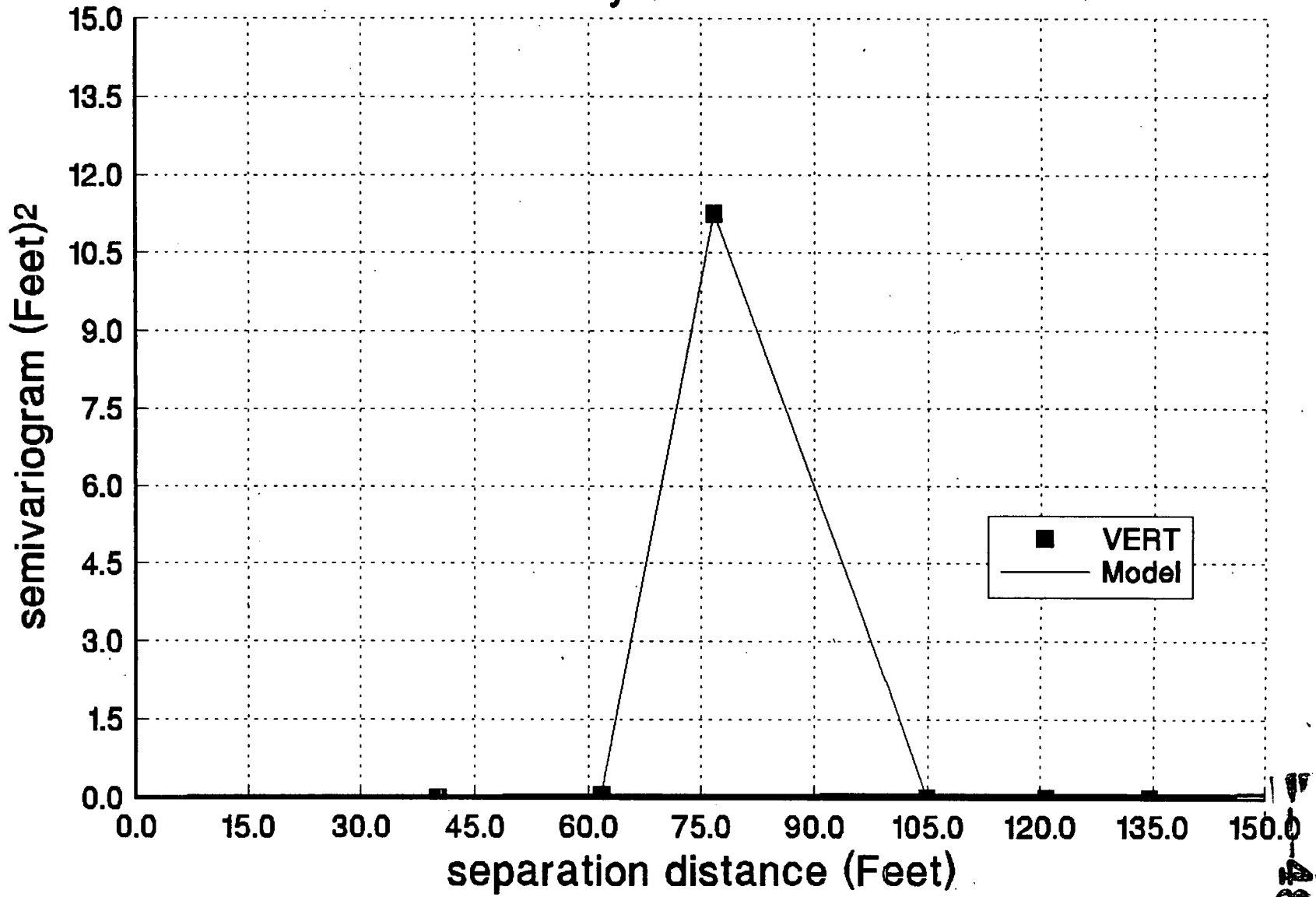


Figure 6 - Horizontal Semivariograms for Steady-State Analysis
 ERAFS1\VOL1:RSAPPSURSDATA\OU-SIPO-37GEOSTAT

-18-

Rev. No.: 0

steady state Vertical



Head Difference vs. Vertical Separation

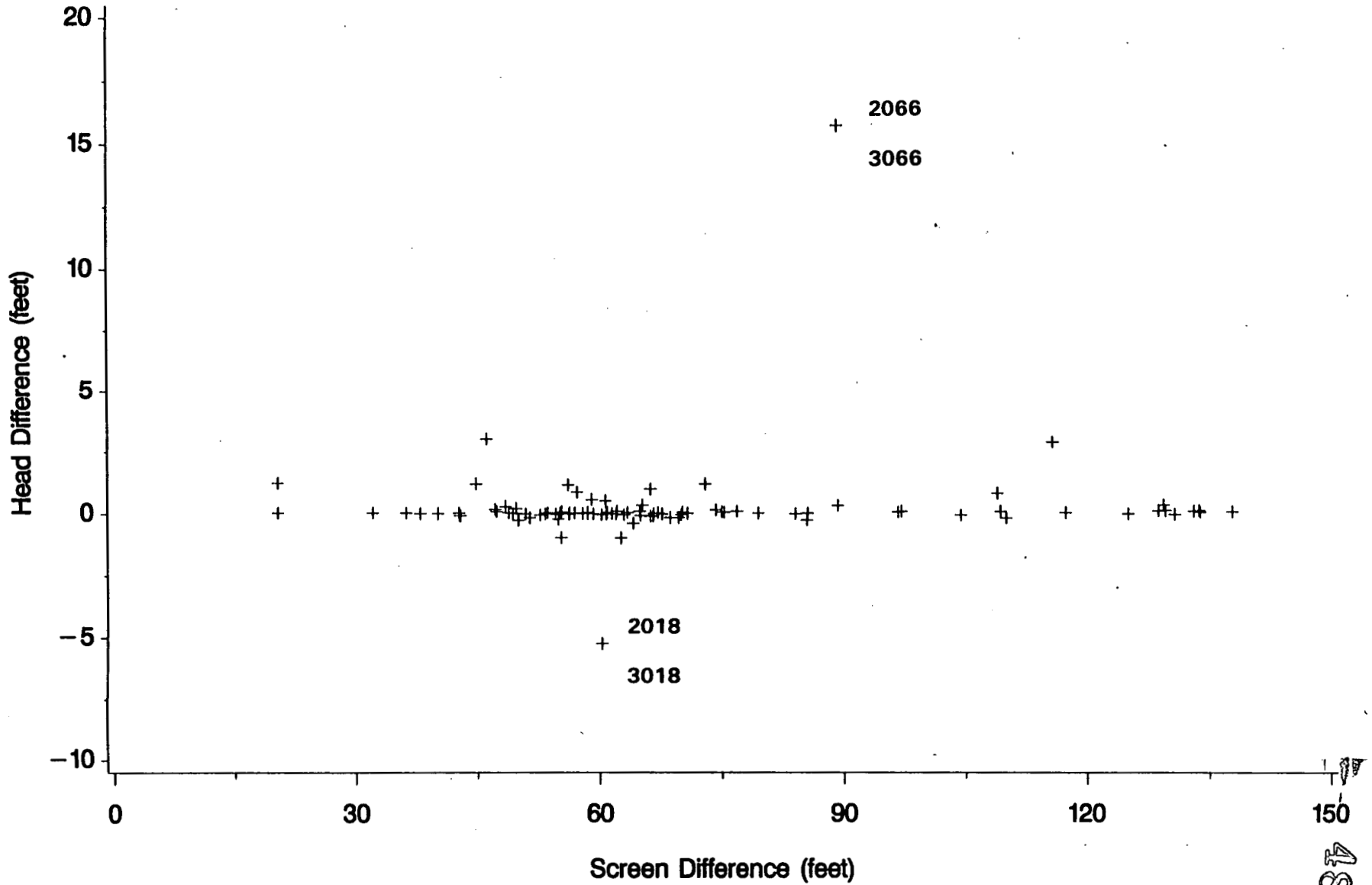


Figure 8 - June, 1993 Head Difference Versus Vertical Separation for Spatially Clustered Wells
 ERAFS\I\VOL1:RSAPPS\RSDATA\
 OU-5\PO-37\GEOSTAT

-20-

Rev. No.: 0

4842

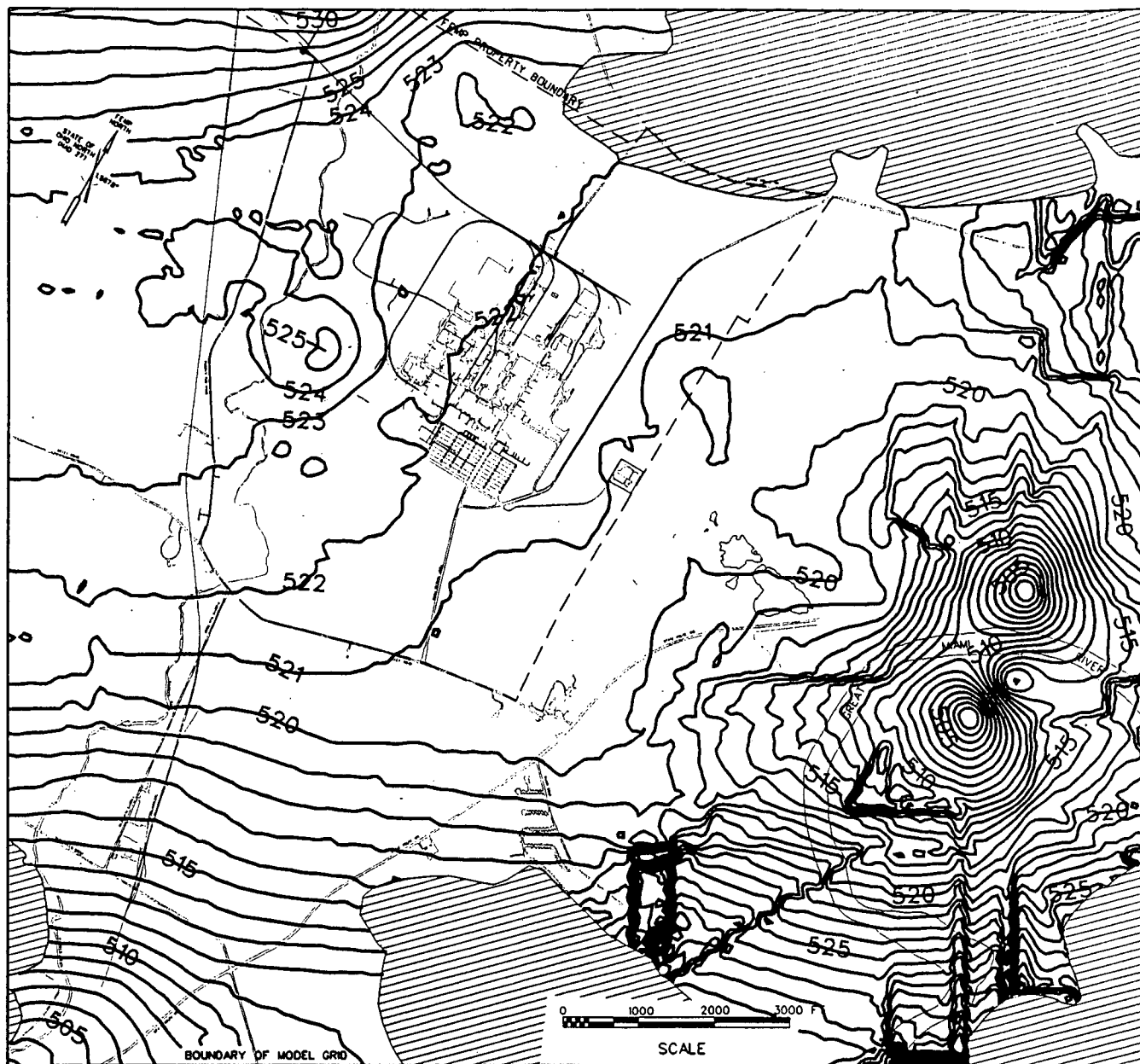


Figure 9 - Estimated Steady-State Water Levels (feet) at 2000 Series Well Level

ERAFS1\VOL1:RSAPPS\RSRDATA\
OU-5\PO-37\GEOSTAT

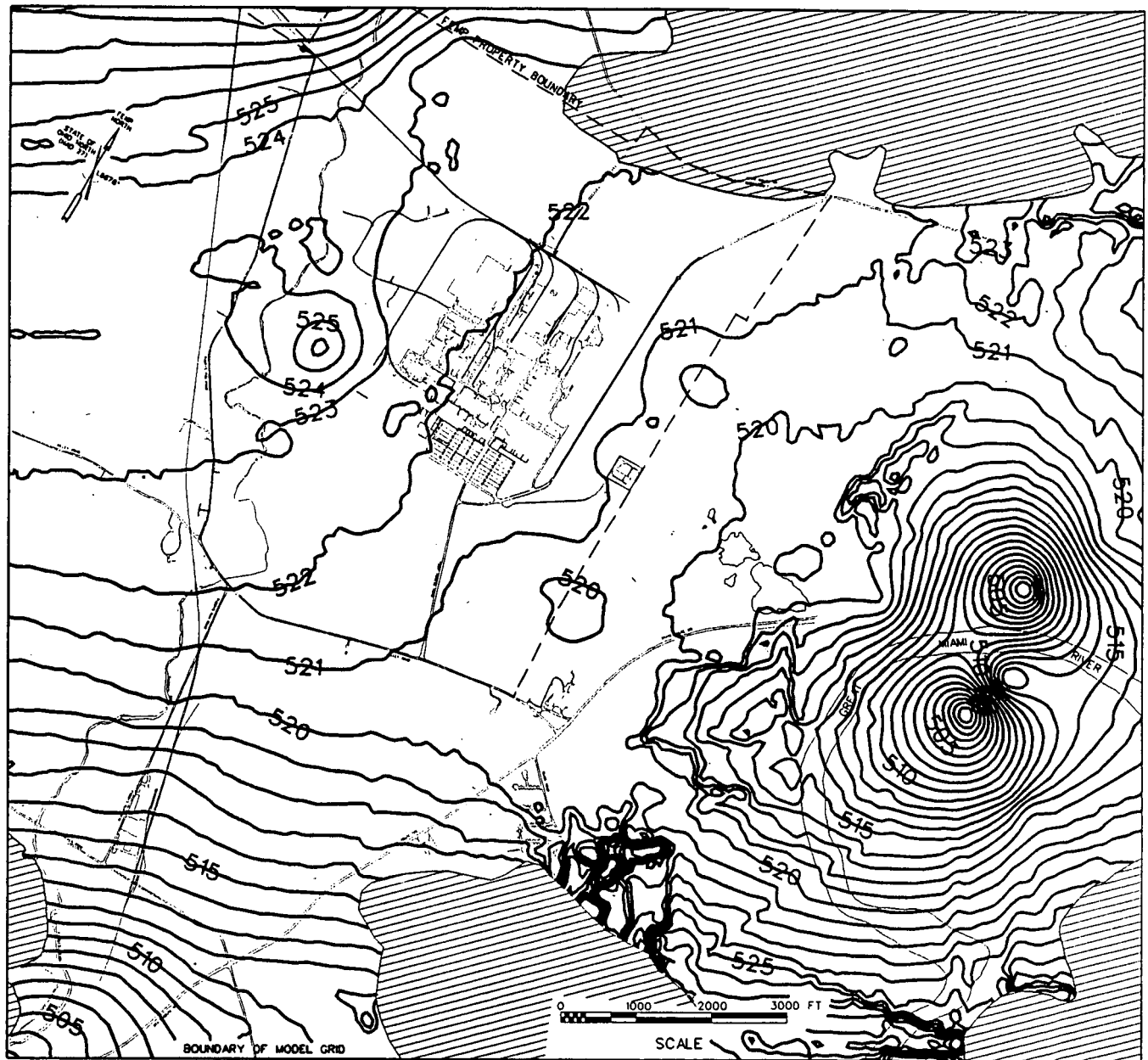


Figure 10 - Estimated Steady-State Water Levels (feet) at 3000 Series Well Level
 ERAFS1\VOL1:RSAPPS\RSDATA\
 OU-5\PO-37\GEOSTAT

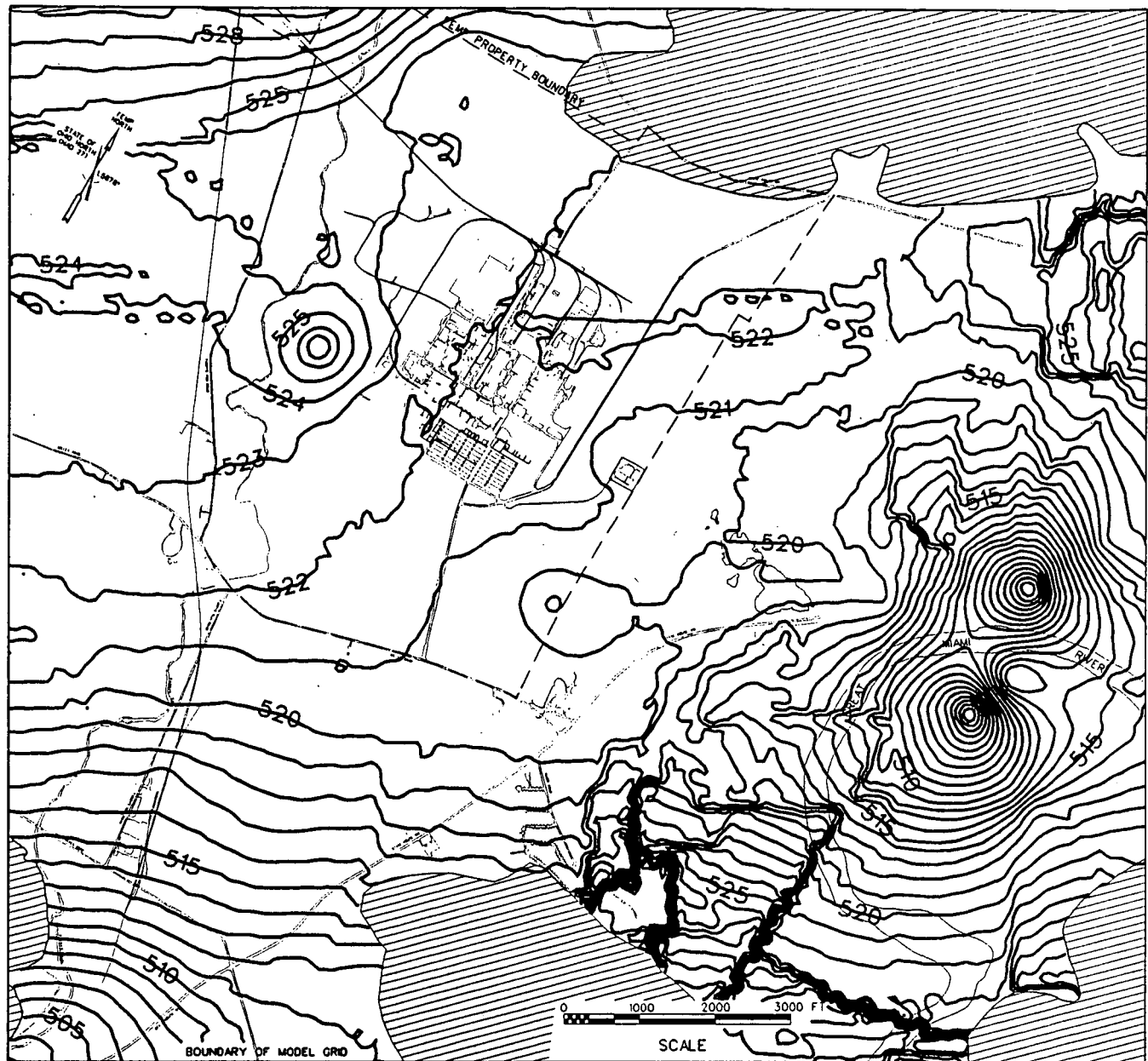


Figure 11 - Estimated Steady-State Water Levels (feet) at 4000 Series Well Level

ERAFS1\VOL1:RSAPPS\RSDATA\
OU-5\PO-37\GEOSTAT

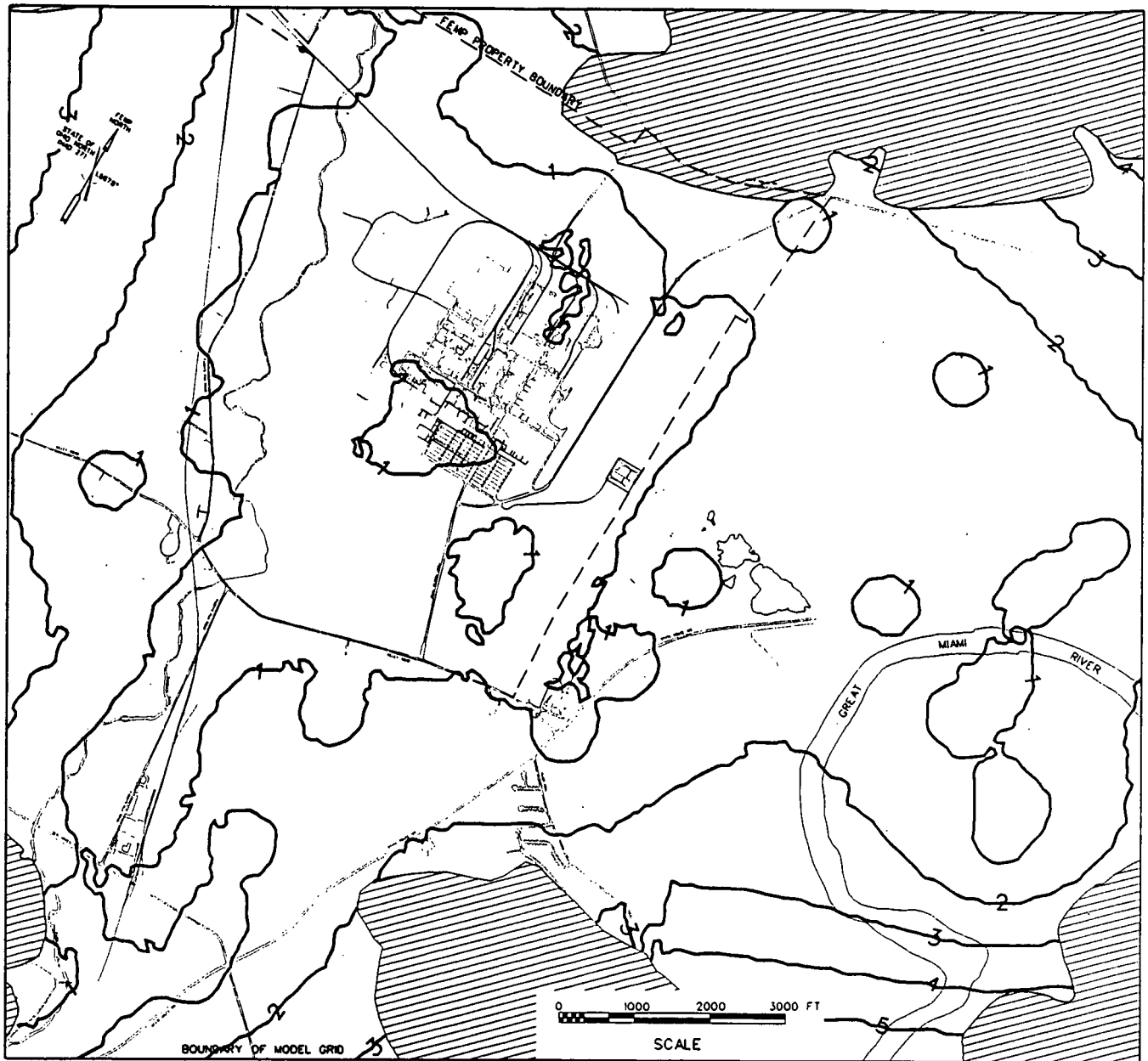


Figure 12 - Statistical Uncertainty (feet) Associated With Steady-State 2000 Series Well Level
 ERAFS1\VOL1\RSAPPS\RSDATA\
 OU-5\PO-37\GEOSTAT

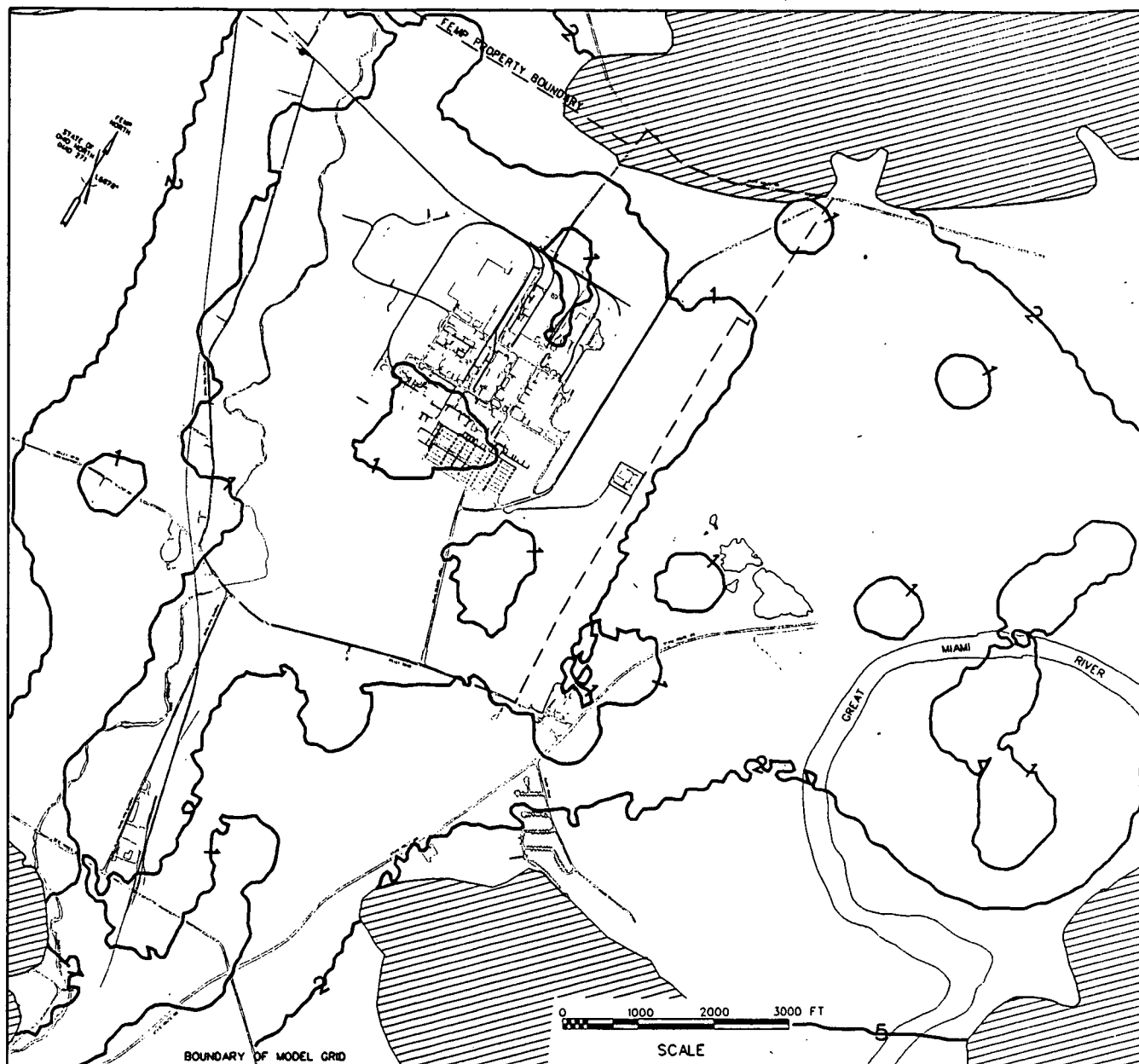


Figure 13 - Statistical Uncertainty (feet) Associated With Steady-State 3000 Series Well Level
 ERAFS1\VOL1:RSAPPS\RSDATA\
 OU-5\PO-37\GEOSTAT

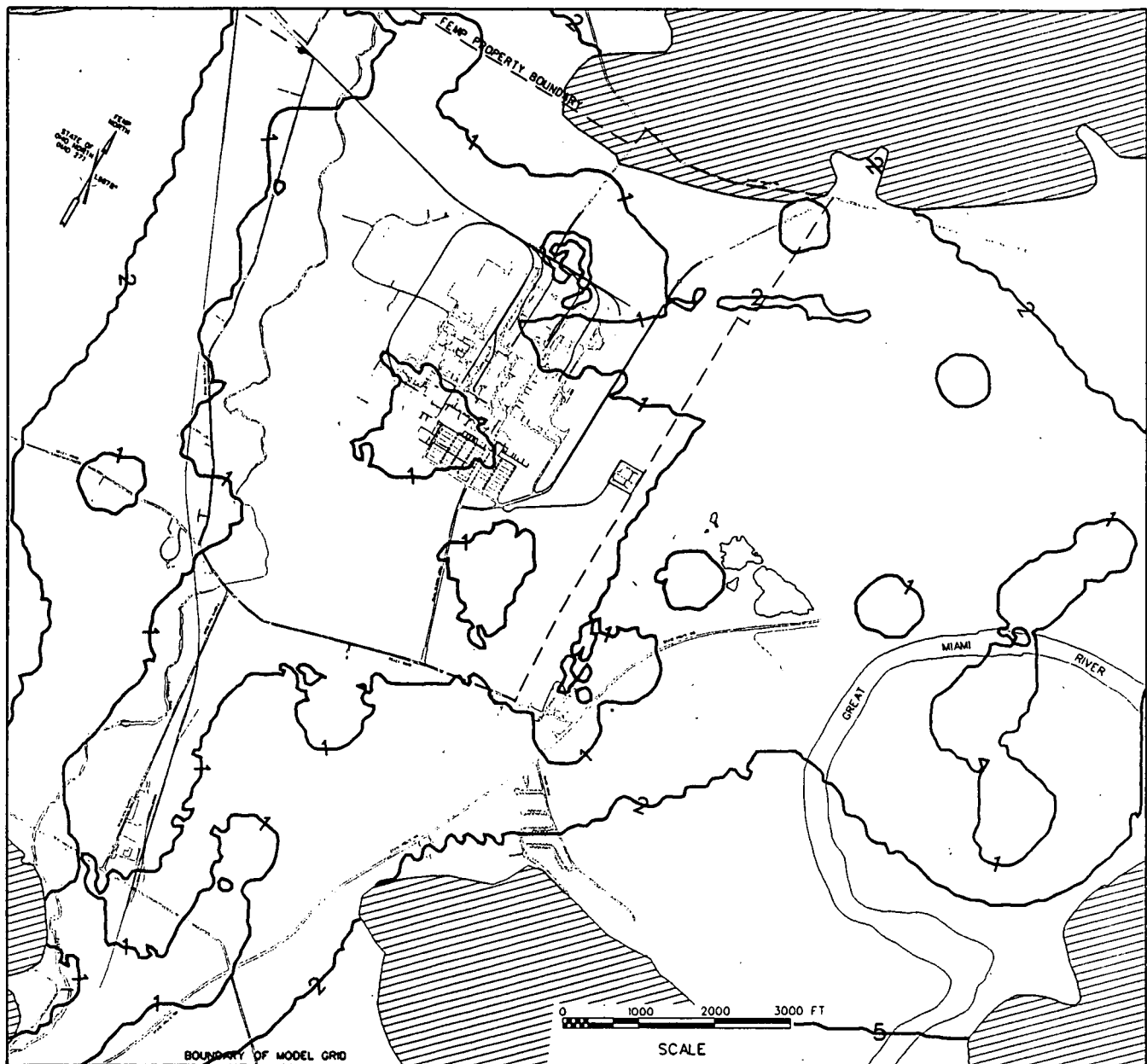


Figure 14 - Statistical Uncertainty (feet) Associated With Steady-State 4000 Series Well Level
 ERAFS1\VOL1:RSAPPS\RSDATA\
 OU-5\PO-37\GEOSTAT

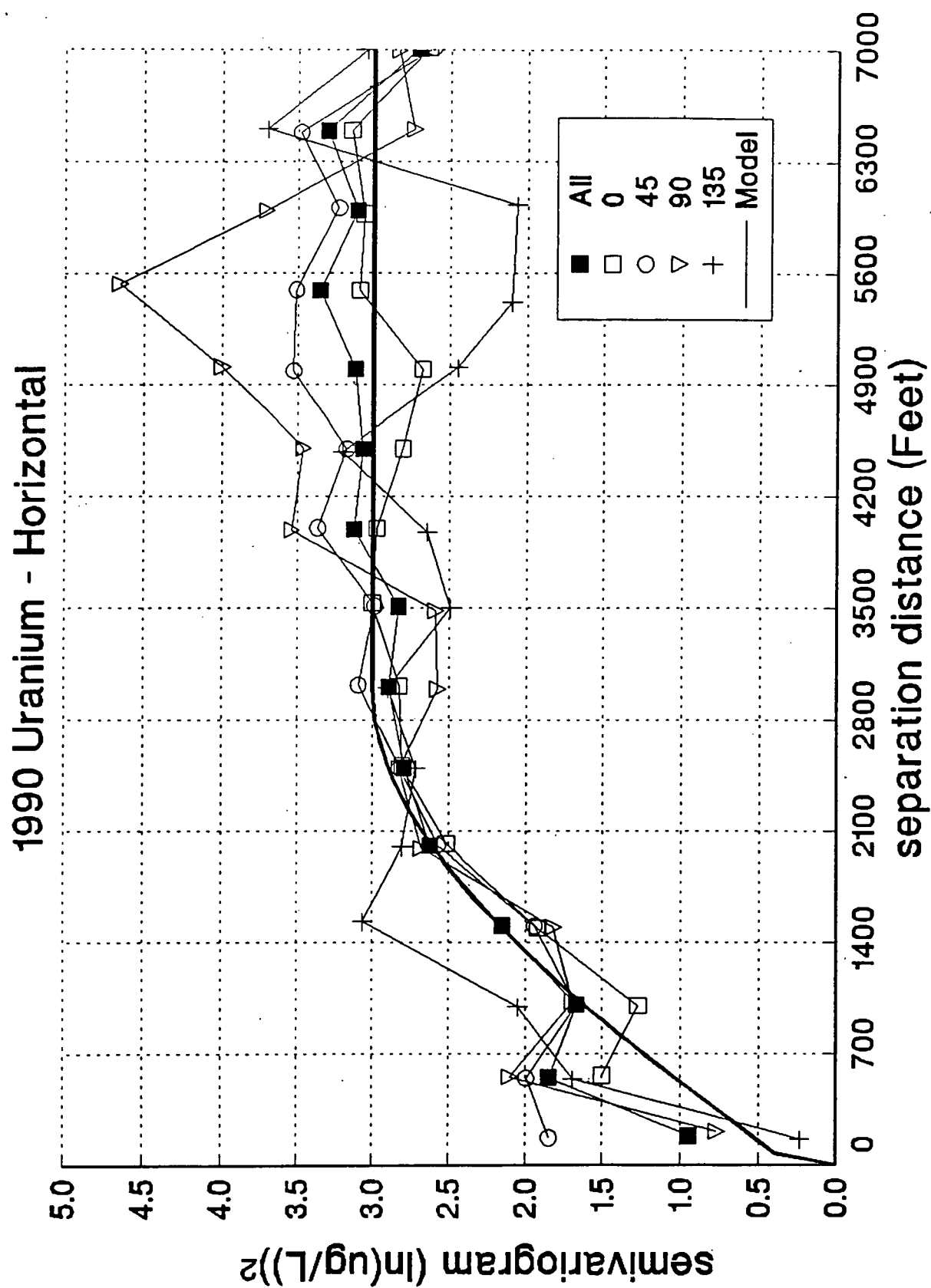


Figure 15 - Horizontal Semivariograms for Log-Transformed 1990 Average Uranium Concentrations
 ERAFS1\VOL1:RSAPPS\RSDATA\
 OU-5\PO-37\GEOSTAT

1990 Uranium - Vertical

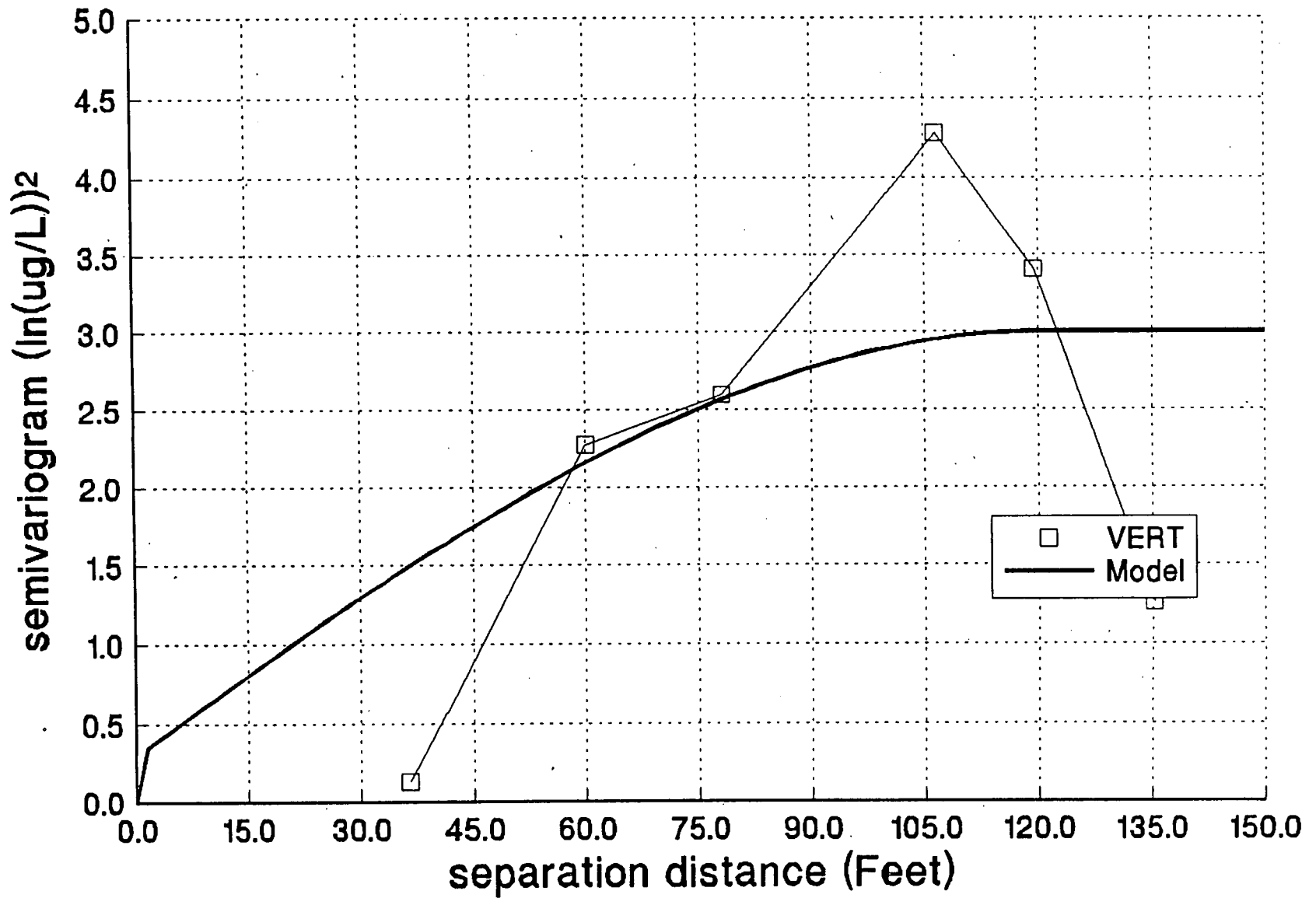


Figure 16 - Vertical Semivariogram for Log-Transformed 1990 Average Uranium Concentrations
 ERAFSI\VOL1:RSAPPS\RSADATA\
 OU-5\PO-37\GEOSTAT

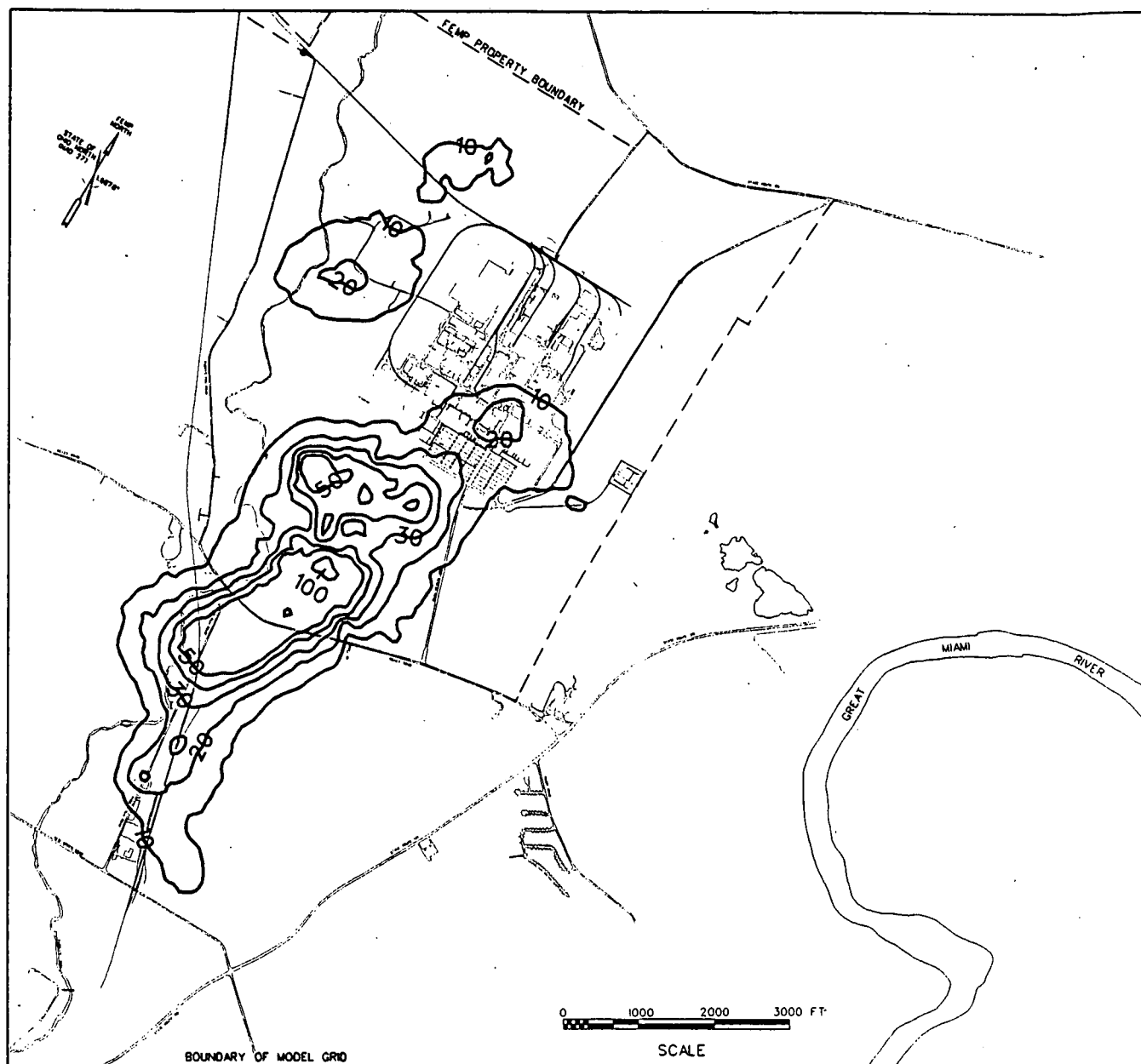


Figure 17 - Estimated 1990 Uranium Concentrations ($\mu\text{g/L}$) at 2000 Series Well Level
ERAFS1\VOL1:RSAPPS\RSDATA\
OU-5\PO-37\GEOSTAT

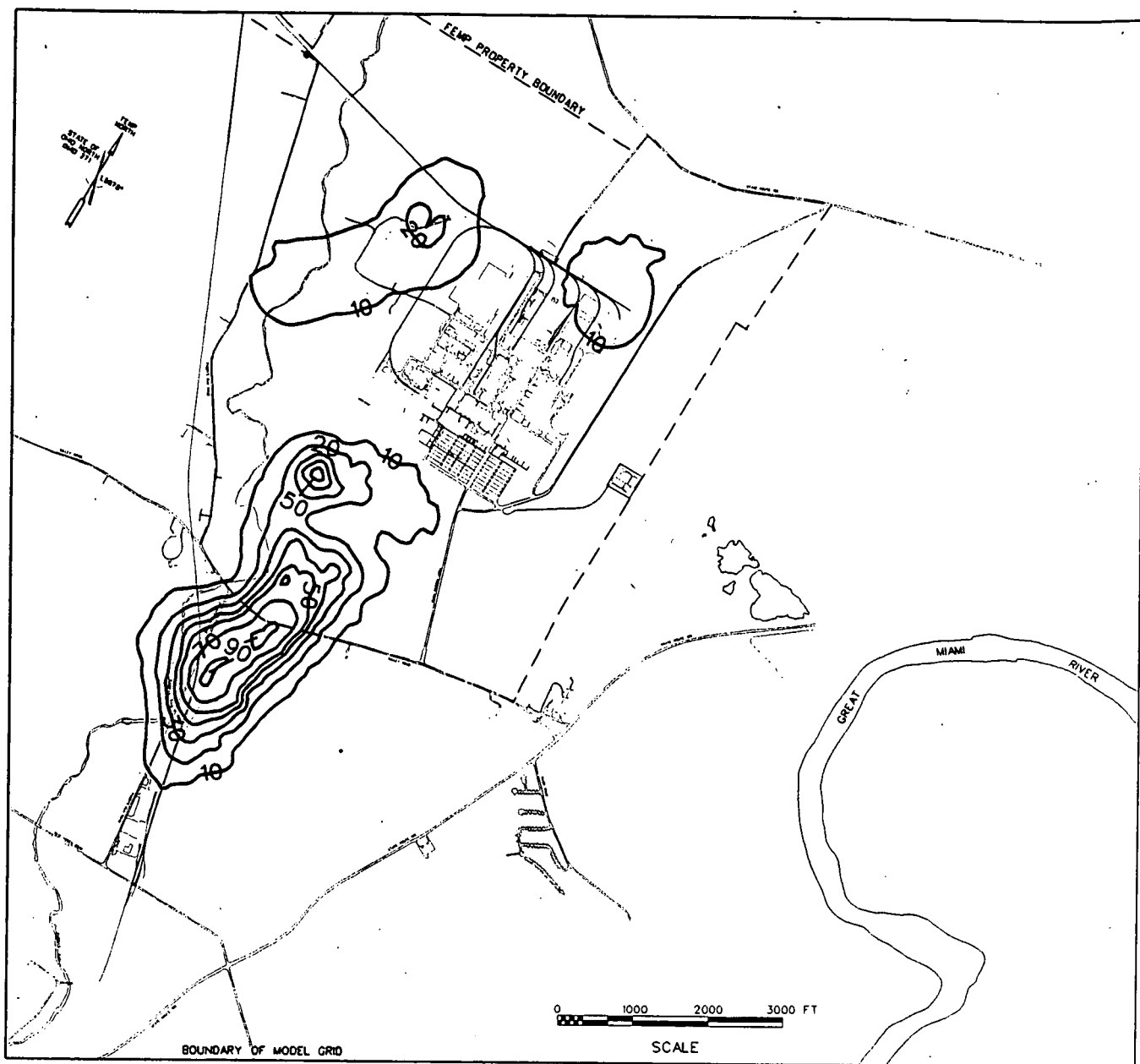


Figure 18 - Estimated 1990 Uranium Concentrations ($\mu\text{g/L}$) at 3000 Series Well Level
 ERAFS\VOL1:RSAPPS\RSDATA\
 OU-5\PO-37\GEOSTAT

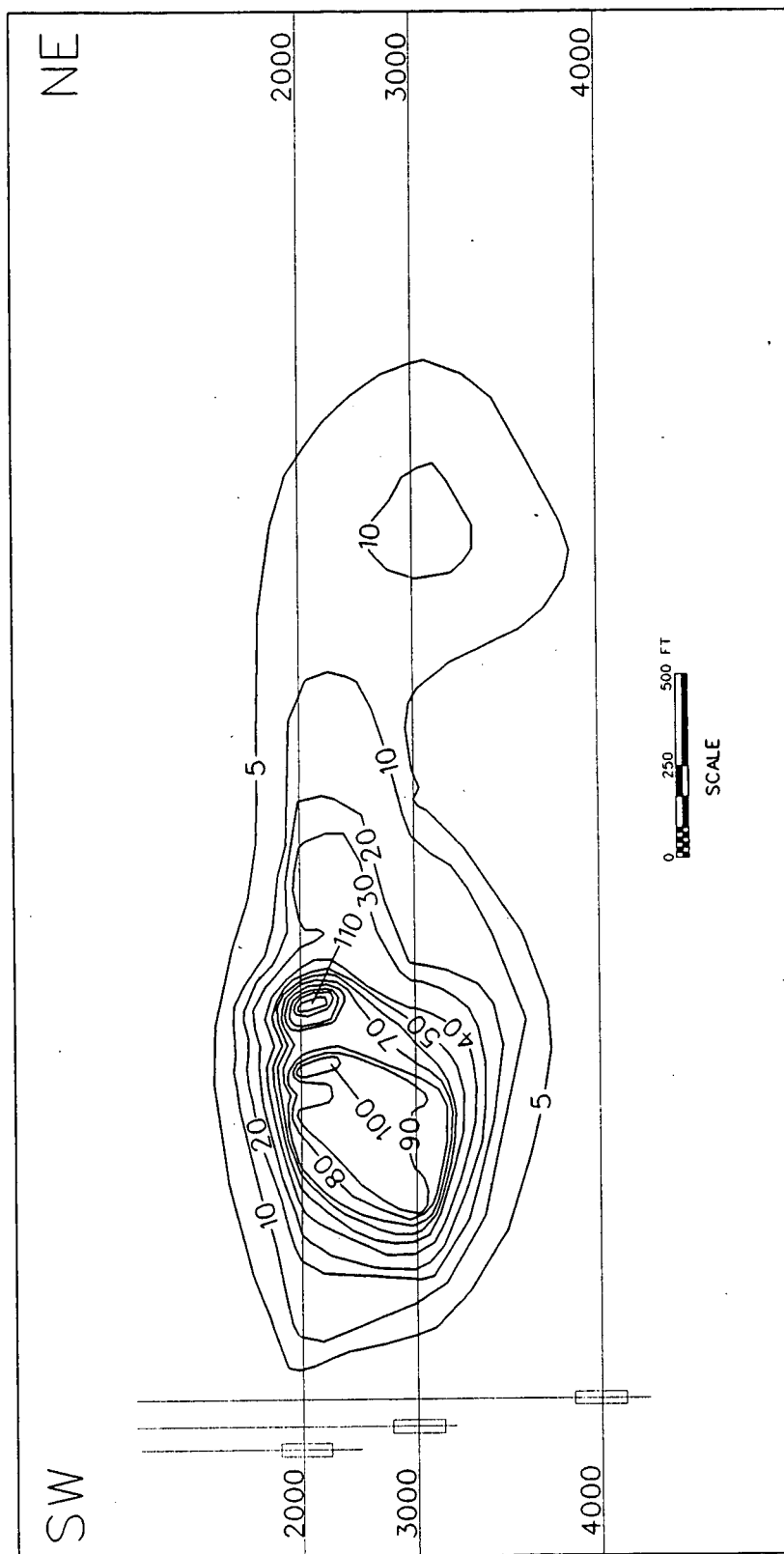


Figure 19 - Northeast-Southwest Vertical Cross-Section of 1990 Uranium Concentrations ($\mu\text{g/L}$)
 ERAFS1\VOL1:RSAPPS\RSDATA\
 OU-5\PO-37\GEOSTAT

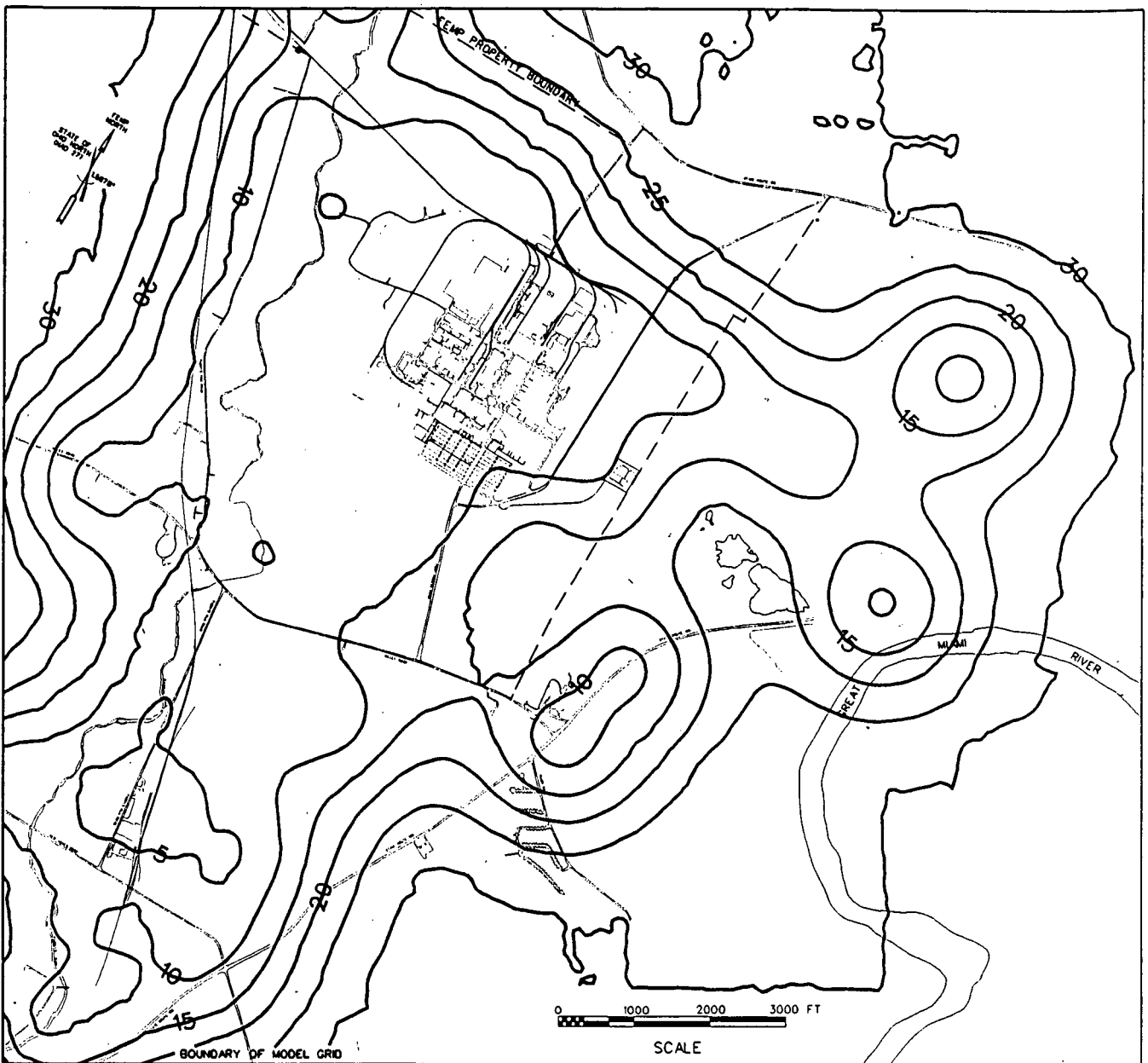


Figure 20 - Multiplicative Statistical Uncertainty Factor Associated with
1990 Uranium Concentration Estimates in 2000 Series Well Levels

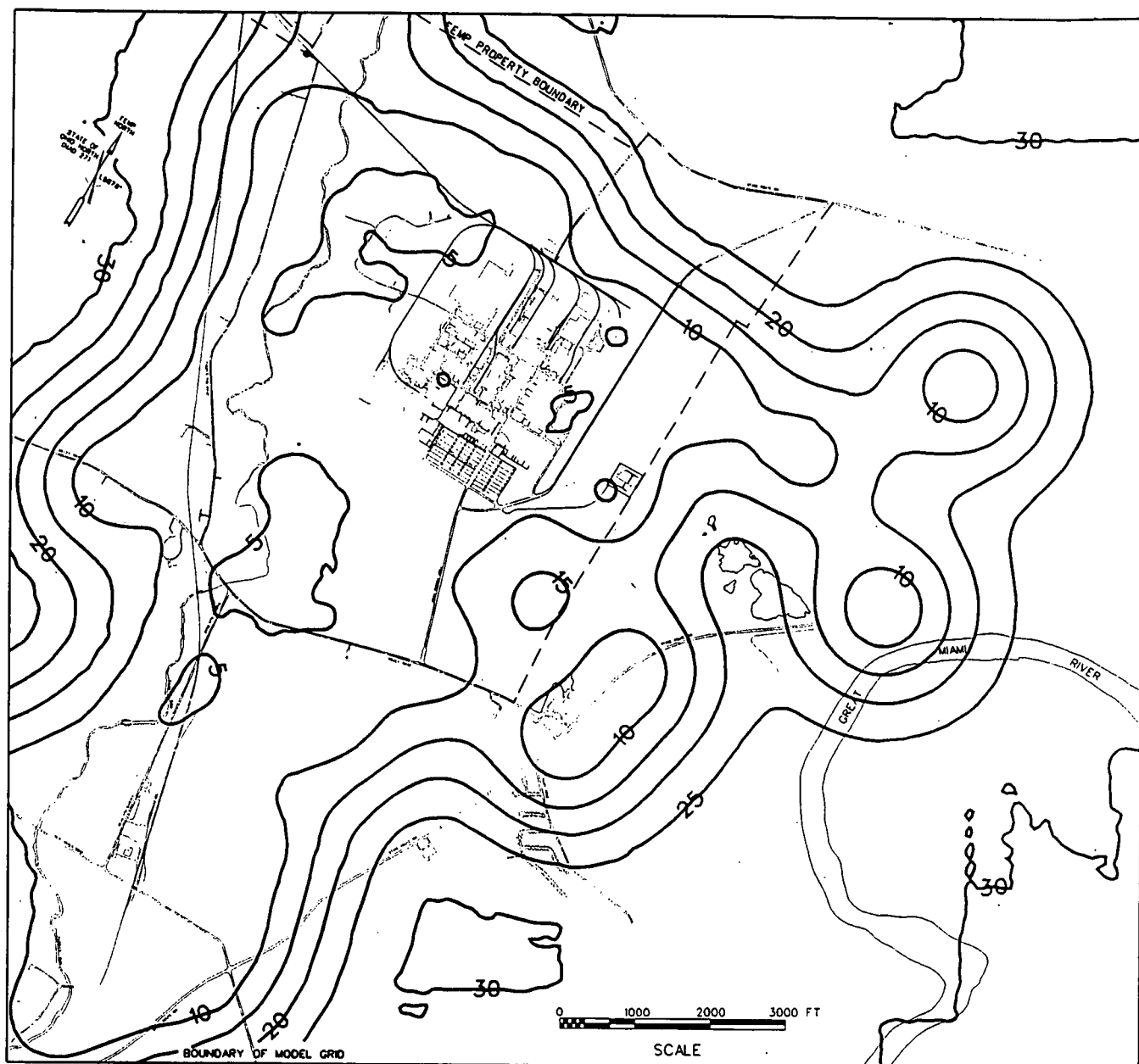


Figure 21 - Multiplicative Statistical Uncertainty Factor Associated with
1990 Uranium Concentration Estimates in 3000 Series Well Levels

1991 Uranium - Horizontal

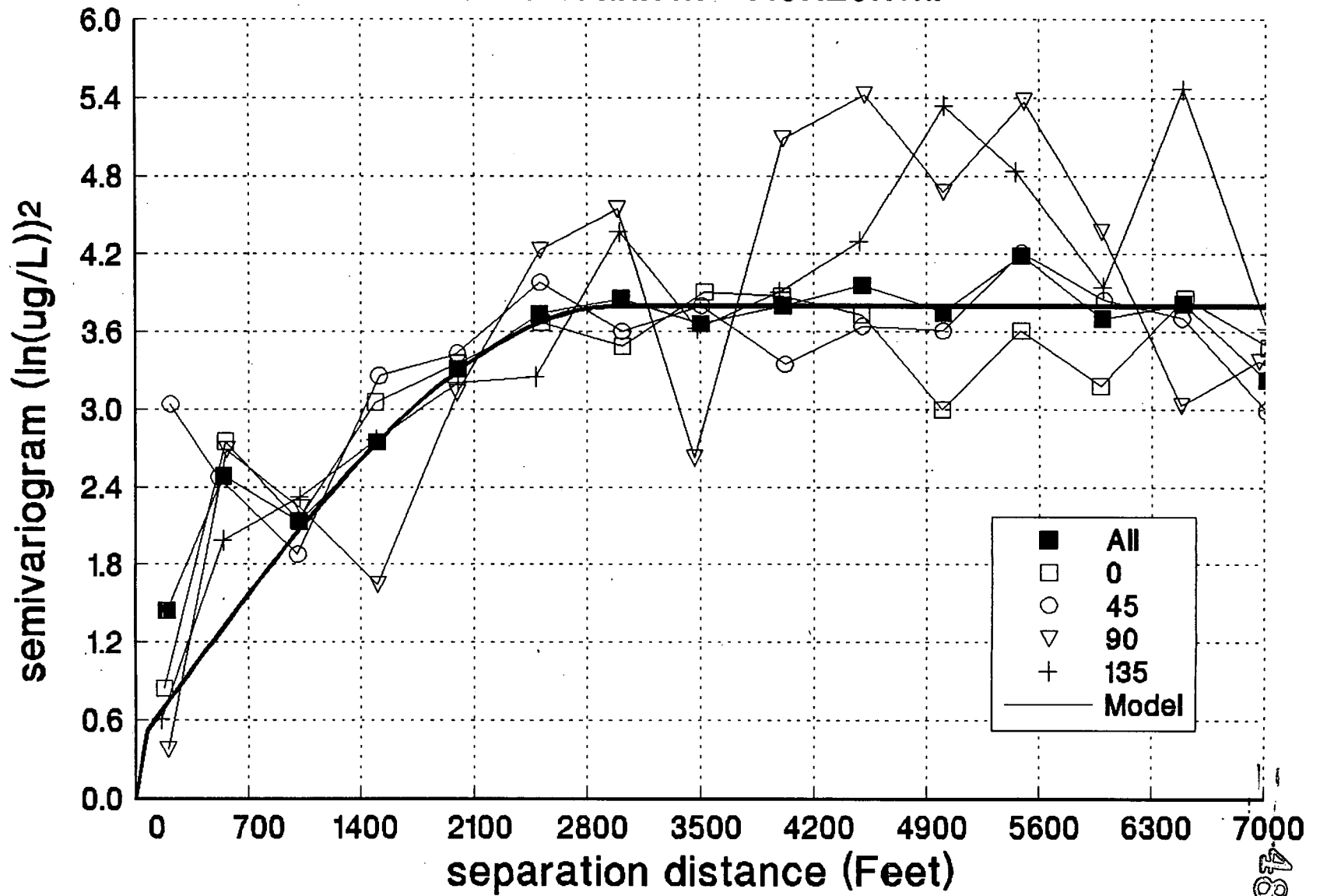


Figure 22 - Horizontal Semivariograms for Log-Transformed 1991 Average Uranium Concentrations
 ERAFSLVOL1:RSAPSRSDATA\OU-SIPO-37GHOSTAT

4842

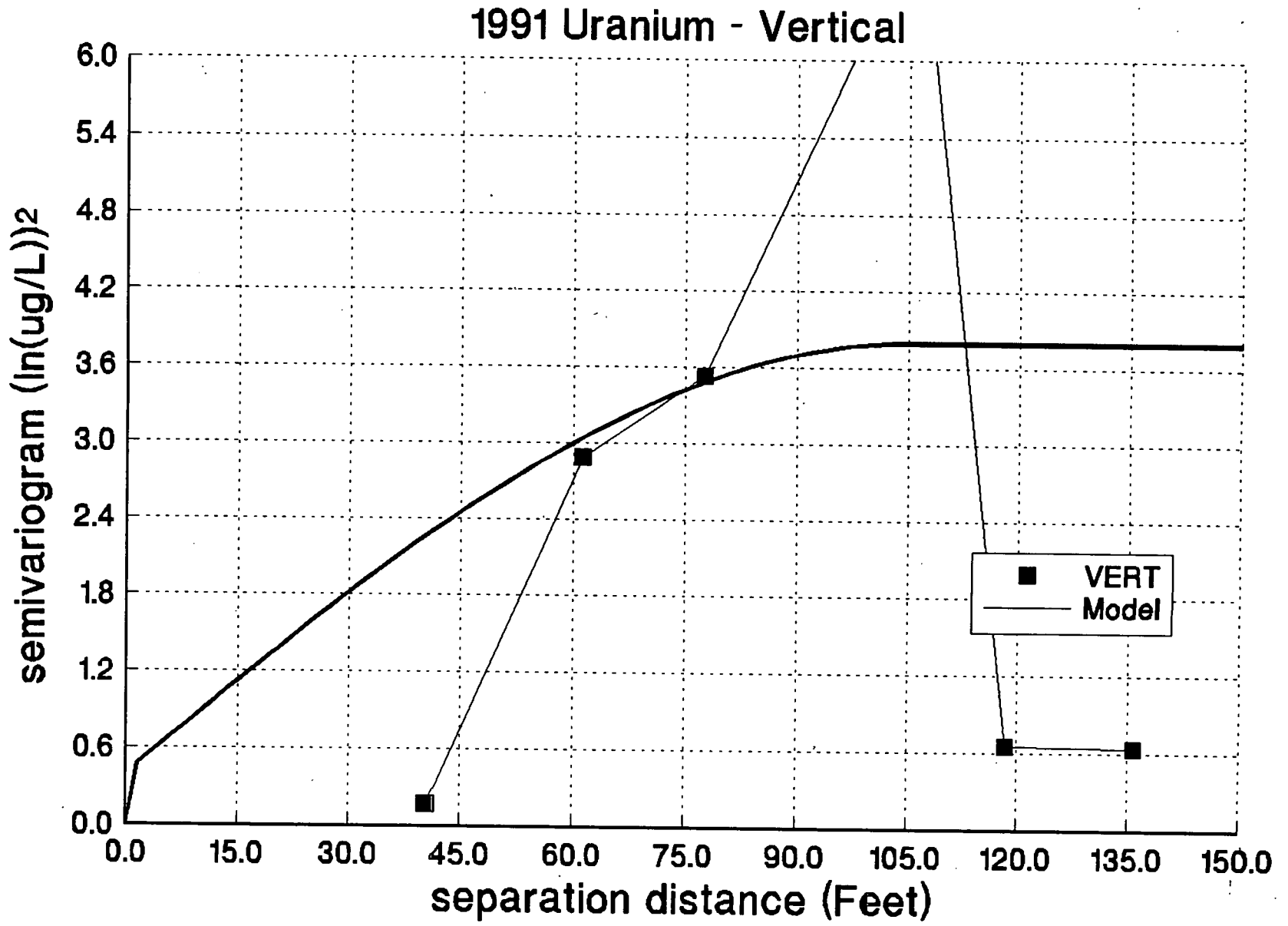


Figure 23 - Vertical Semivariogram for Log-Transformed 1991 Average Uranium Concentrations
 ERAF51VOL1:RSAPSRSDATA\
 OU-5PO-37GEOSTAT

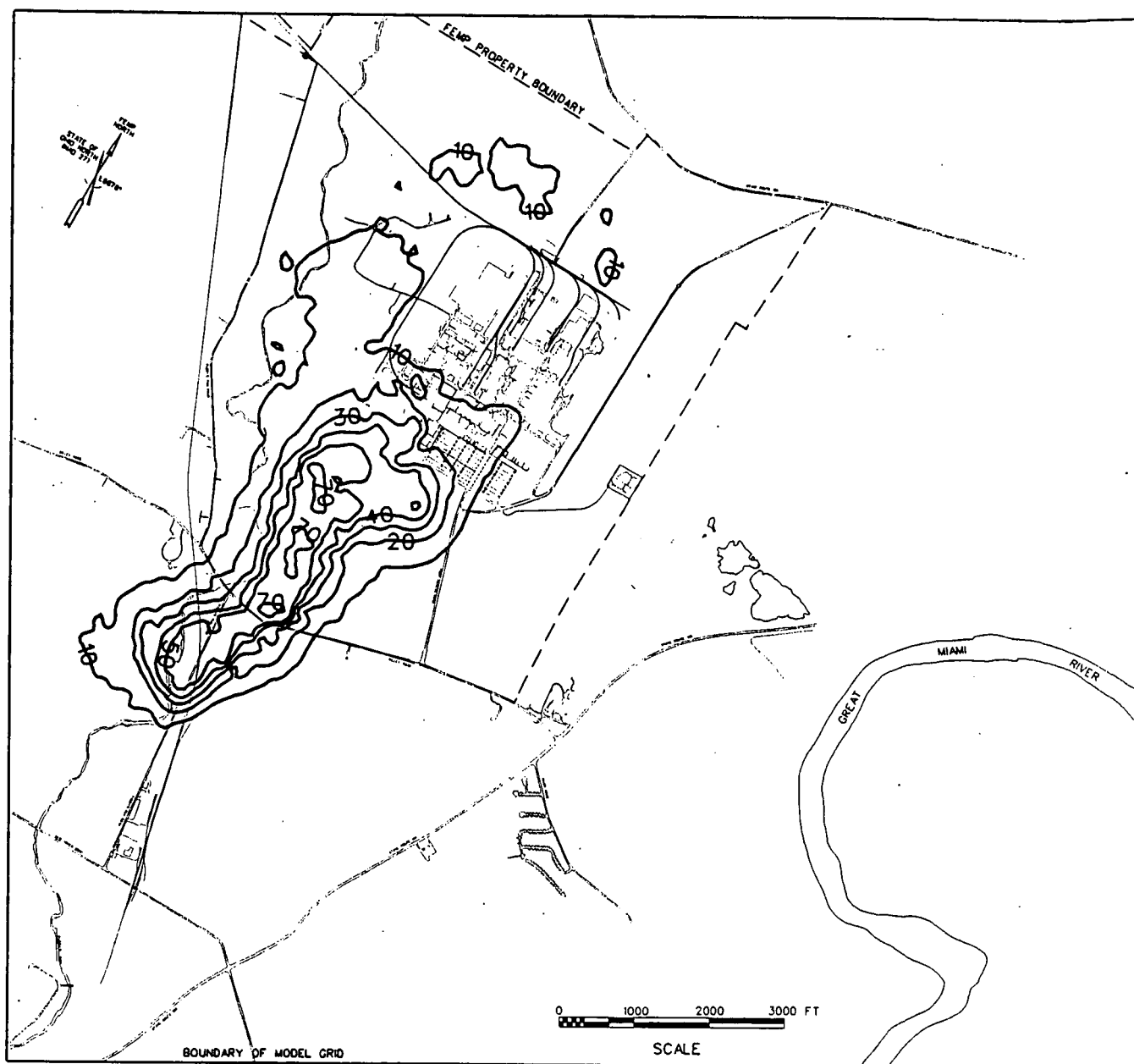


Figure 24 - Estimated 1991 Uranium Concentrations ($\mu\text{g/L}$) at 2000 Series Well Level
 ERAFS1\VOL1:RSAPPS\RSDATA\
 OU-5\PO-37\GEOSTAT

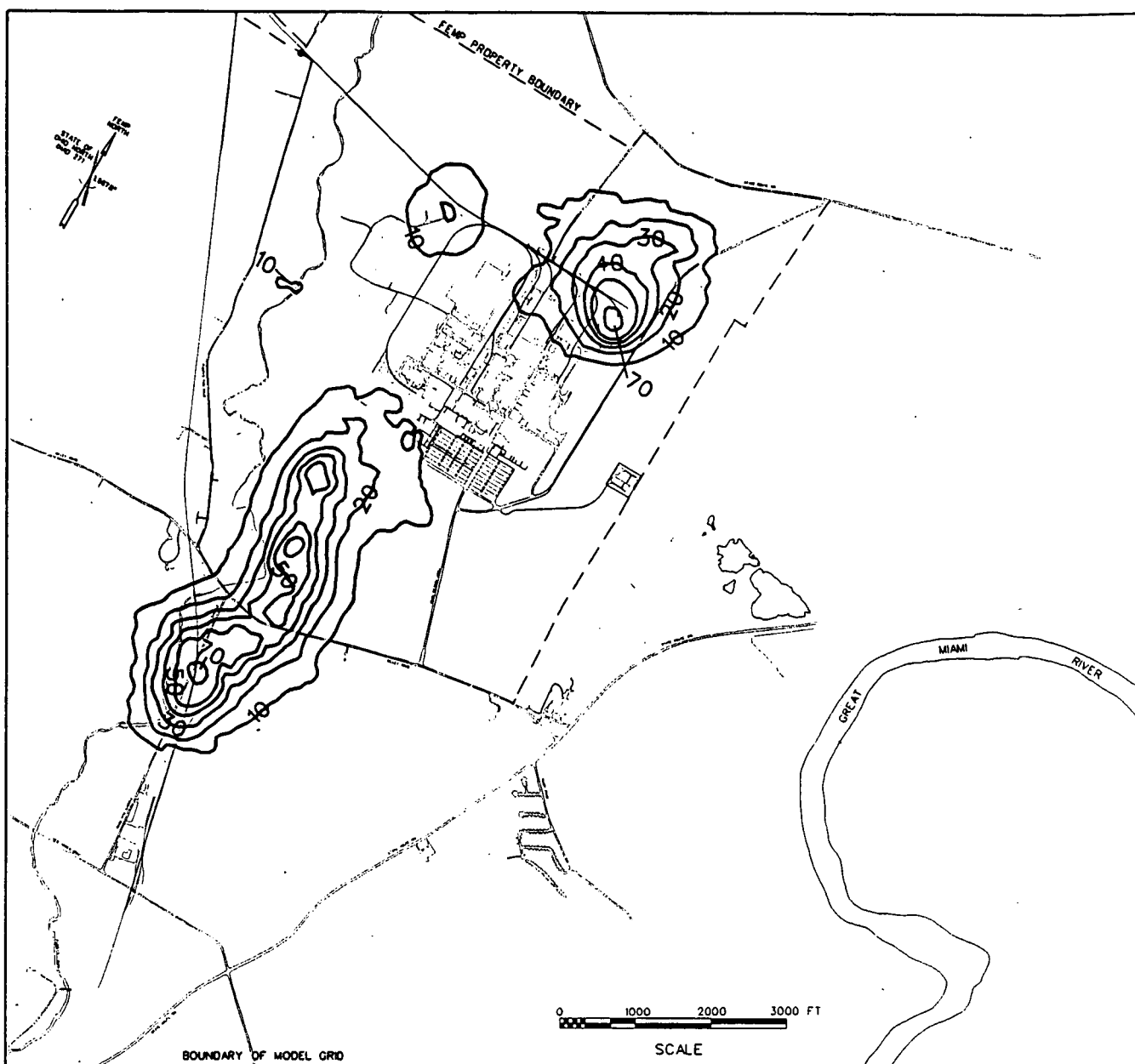


Figure 25 - Estimated 1991 Uranium Concentrations (µg/L) at 3000 Series Well Level
 ERAFS\VOL1:RSAPPS\RSDATA\
 OU-5\PO-37\GEOSTAT

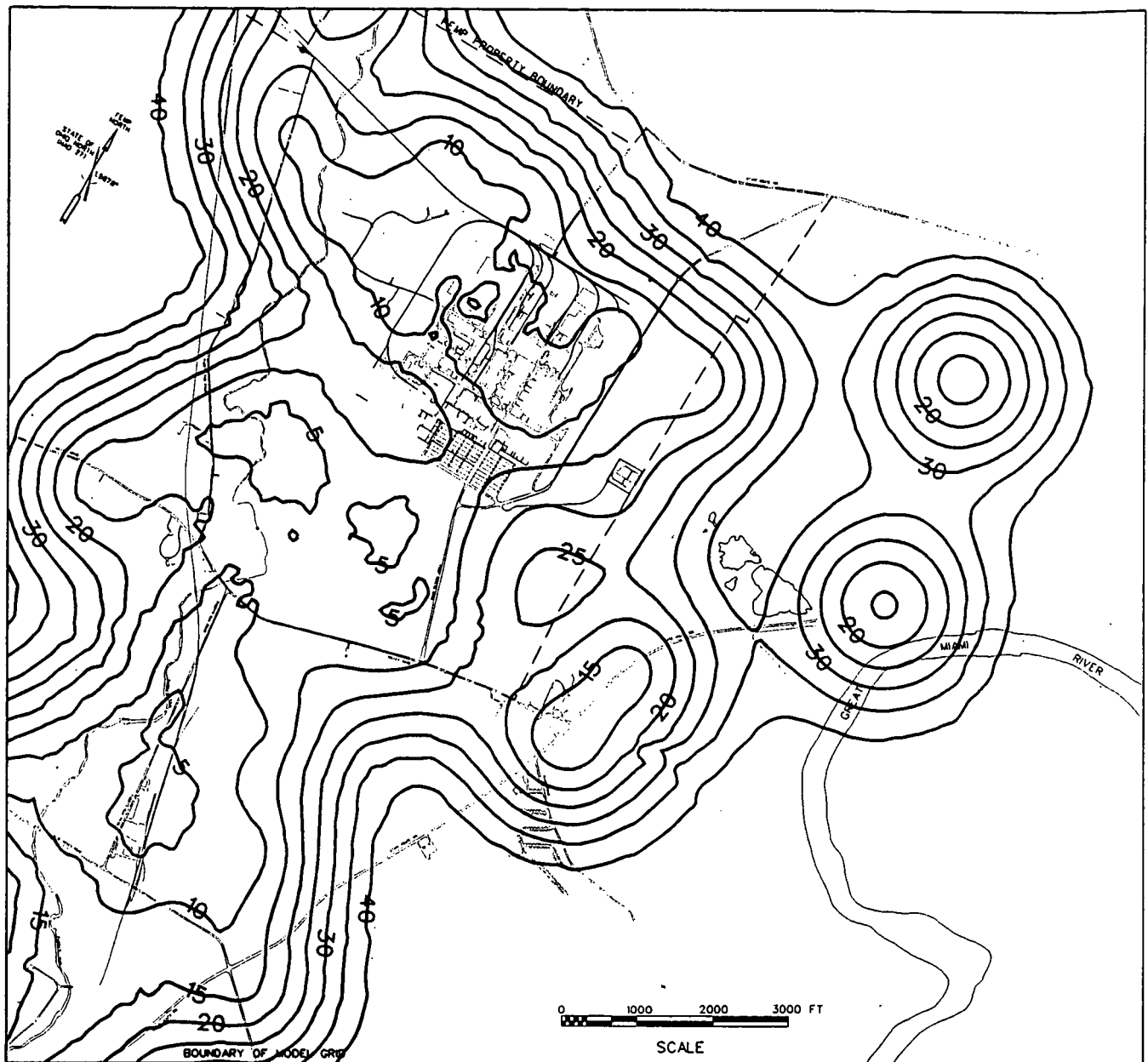


Figure 26 - Multiplicative Statistical Uncertainty Factor Associated with
1991 Uranium Concentration Estimates in 2000 Series Well Levels

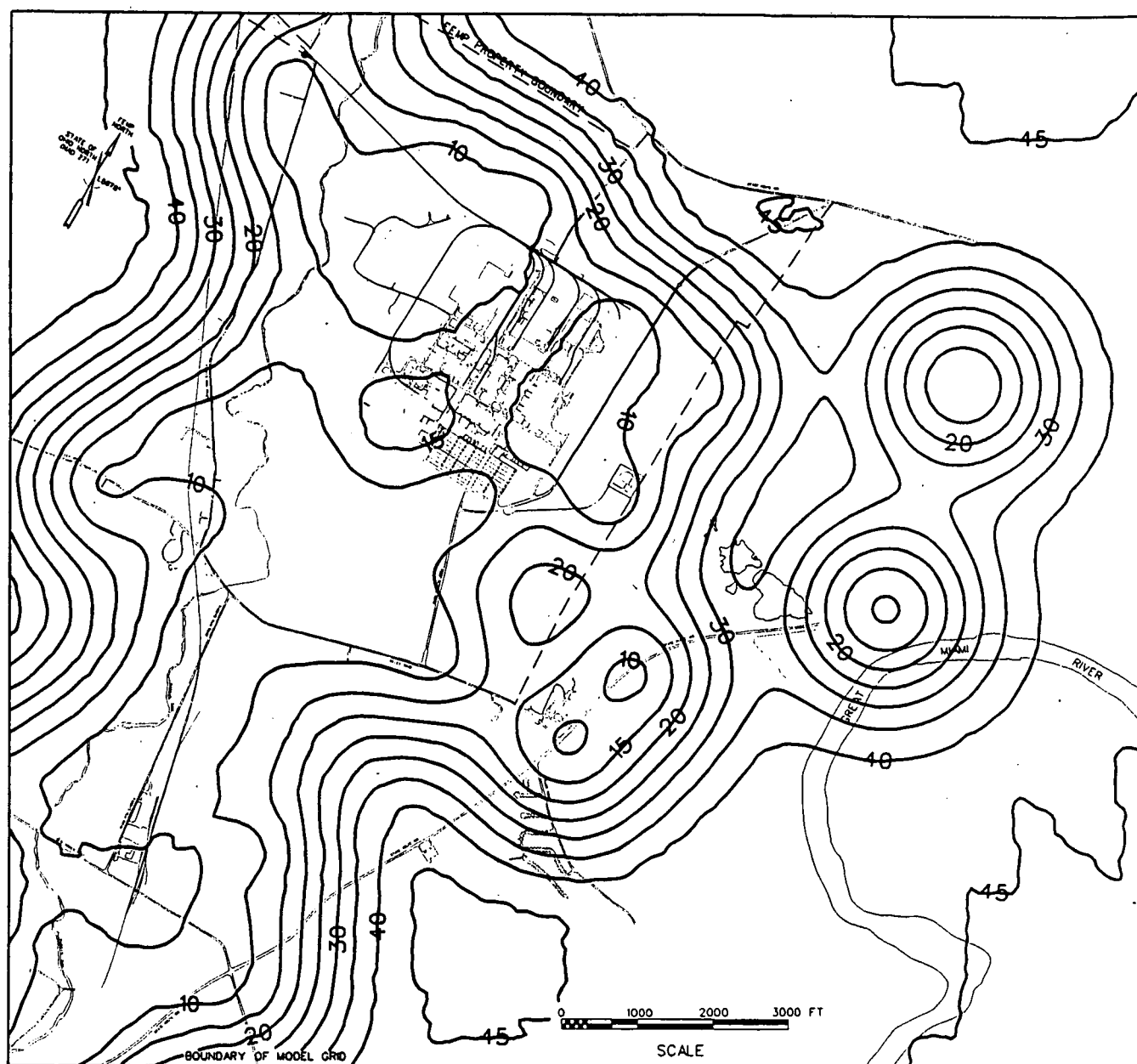


Figure 27 - Multiplicative Statistical Uncertainty Factor Associated with
1991 Uranium Concentration Estimates in 3000 Series Well Levels

1992 Uranium Horizontal

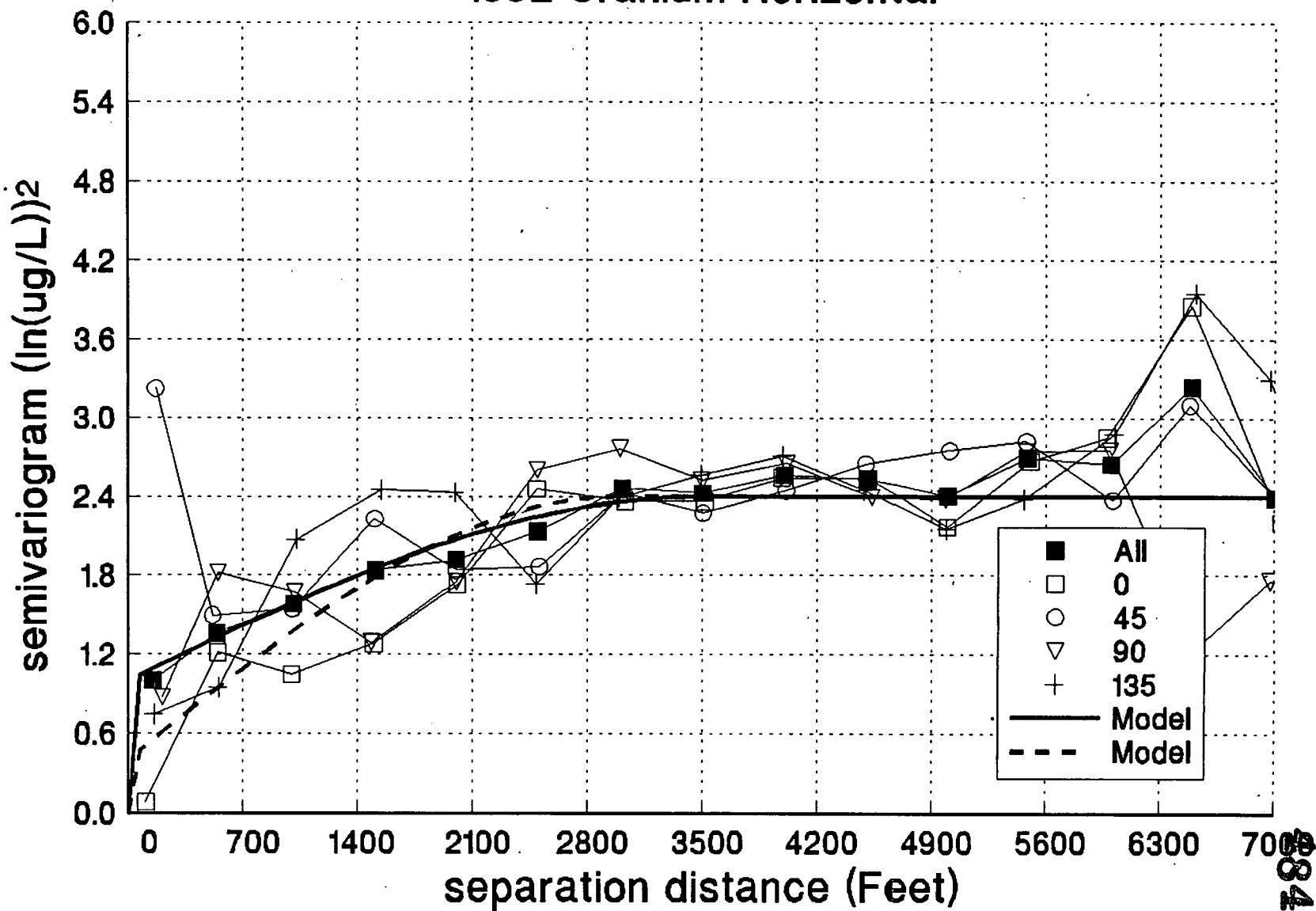


Figure 28 - Horizontal Semivariograms for Log-Transformed 1992 Average Uranium Concentrations
 BRAFSLVOL1:RSAPPSURSDATA\OU-51PO-37GEOSTAT

-40-

Rev. No.: 0

0842

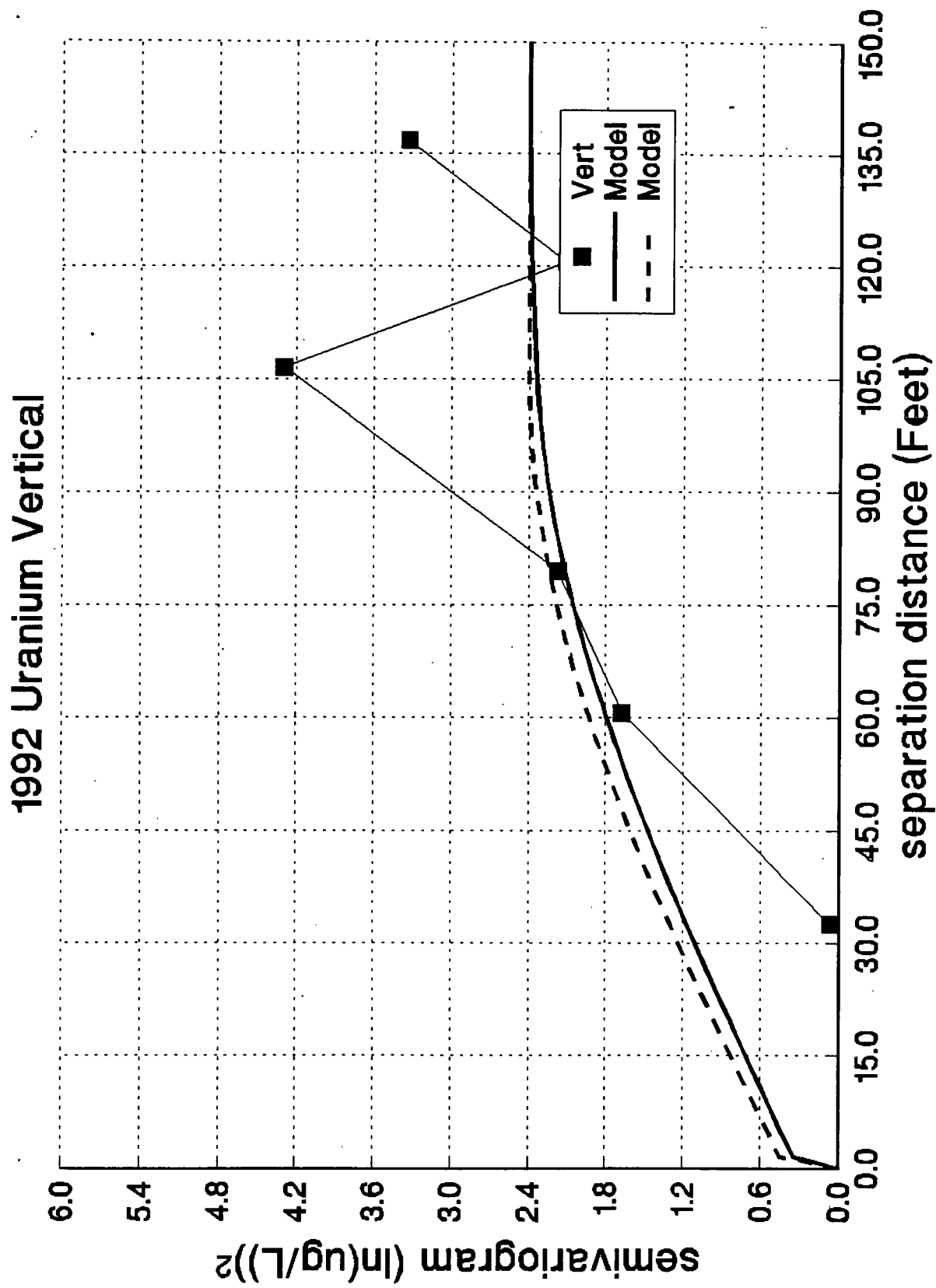


Figure 29 - Vertical Semivariogram for Log-Transformed 1992 Average Uranium Concentrations
 ERAFS1\VOL1:RSAPPS\RSDATA\
 OU-5\PO-37\GEOSTAT

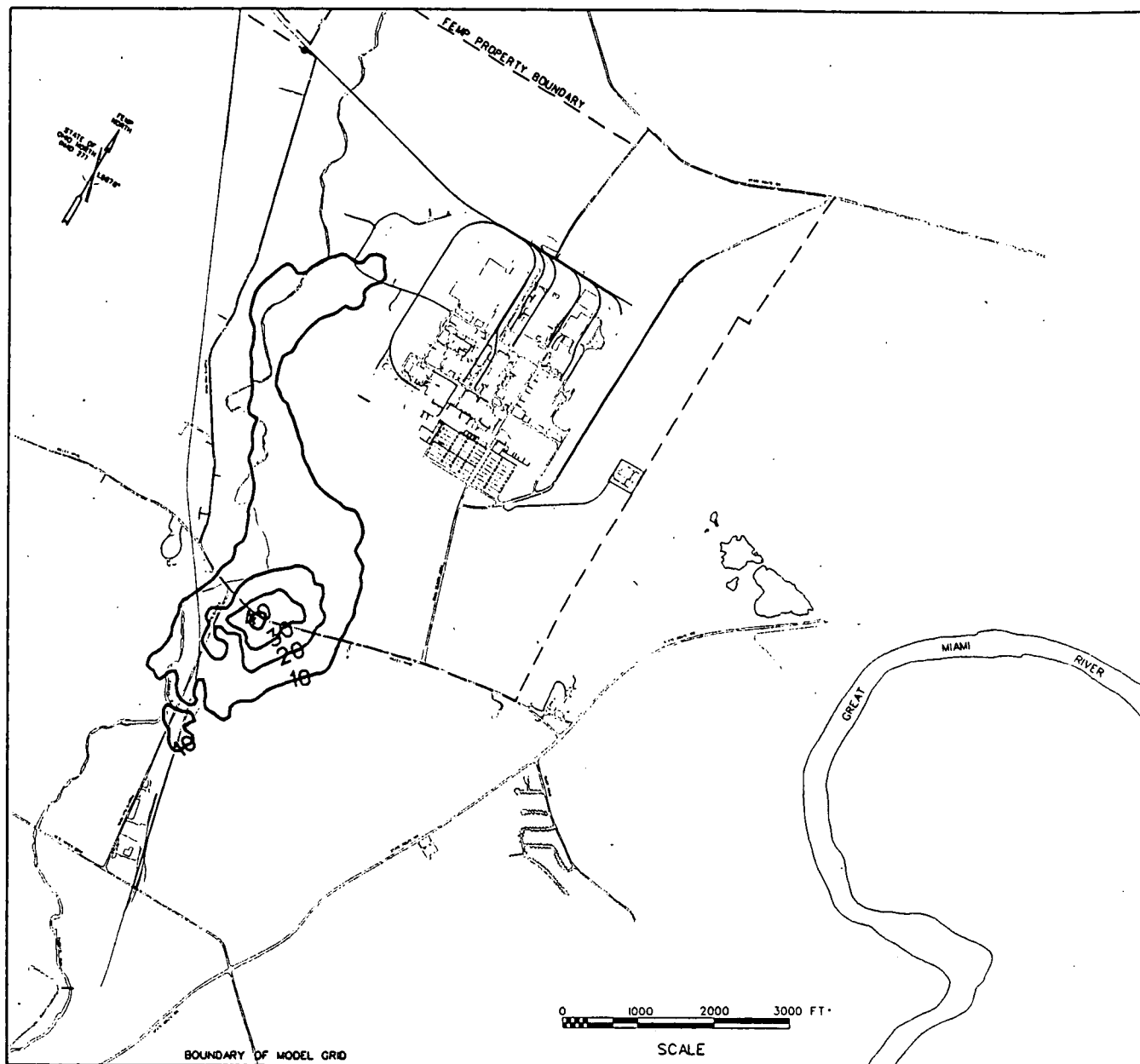


Figure 30 - Estimated 1992 Uranium Concentrations ($\mu\text{g/L}$) at 2000 Series Well Level
ERAFS\VOL1:RSAPPS\RSDATA\
OU-5\PO-37\GEOSTAT

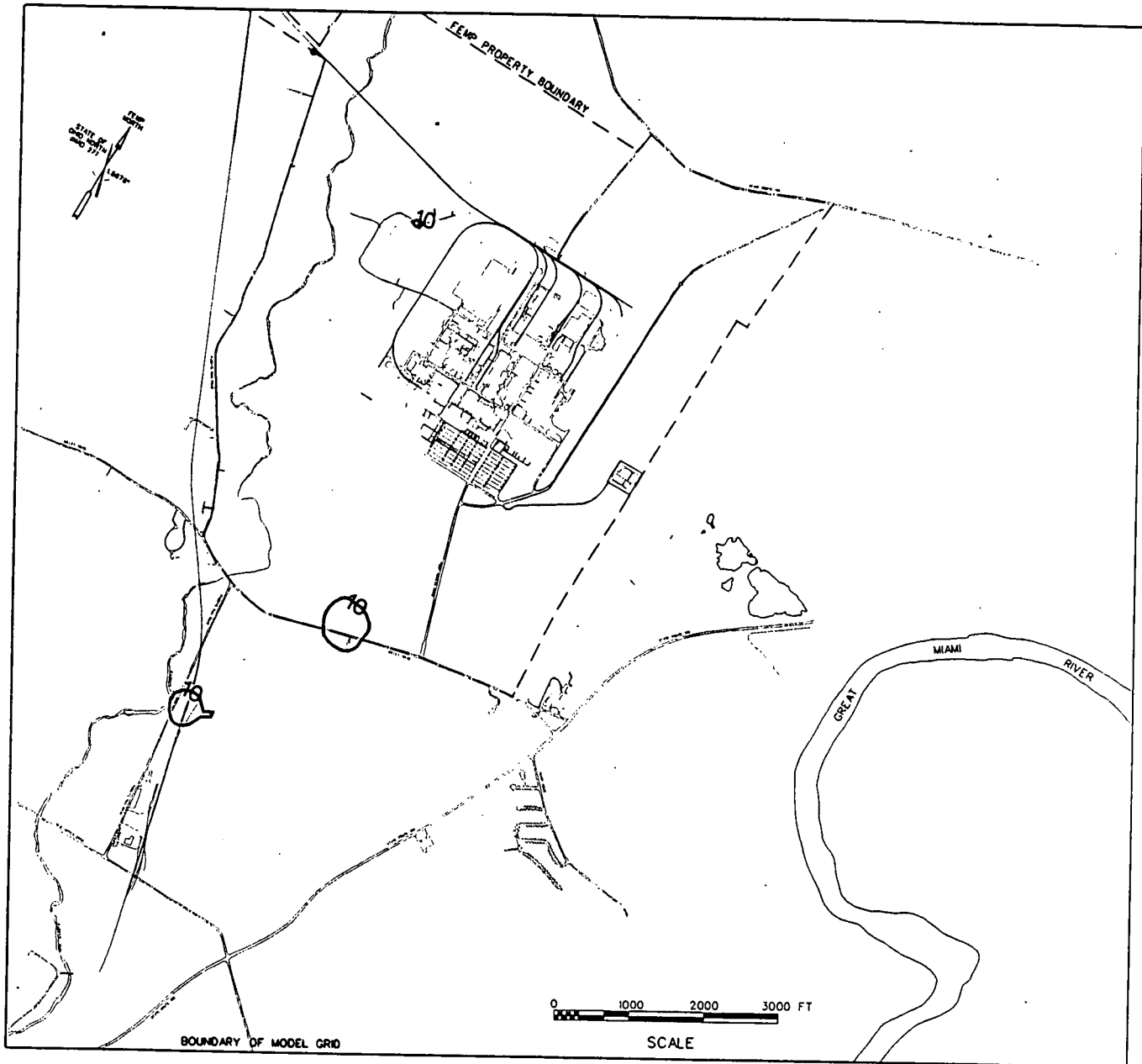


Figure 31 - Estimated 1992 Uranium Concentrations ($\mu\text{g/L}$) at 3000 Series Well Level
 ERAFS1\VOL1:RSAPPS\RSDATA\
 OU-5\PO-37\GEOSTAT

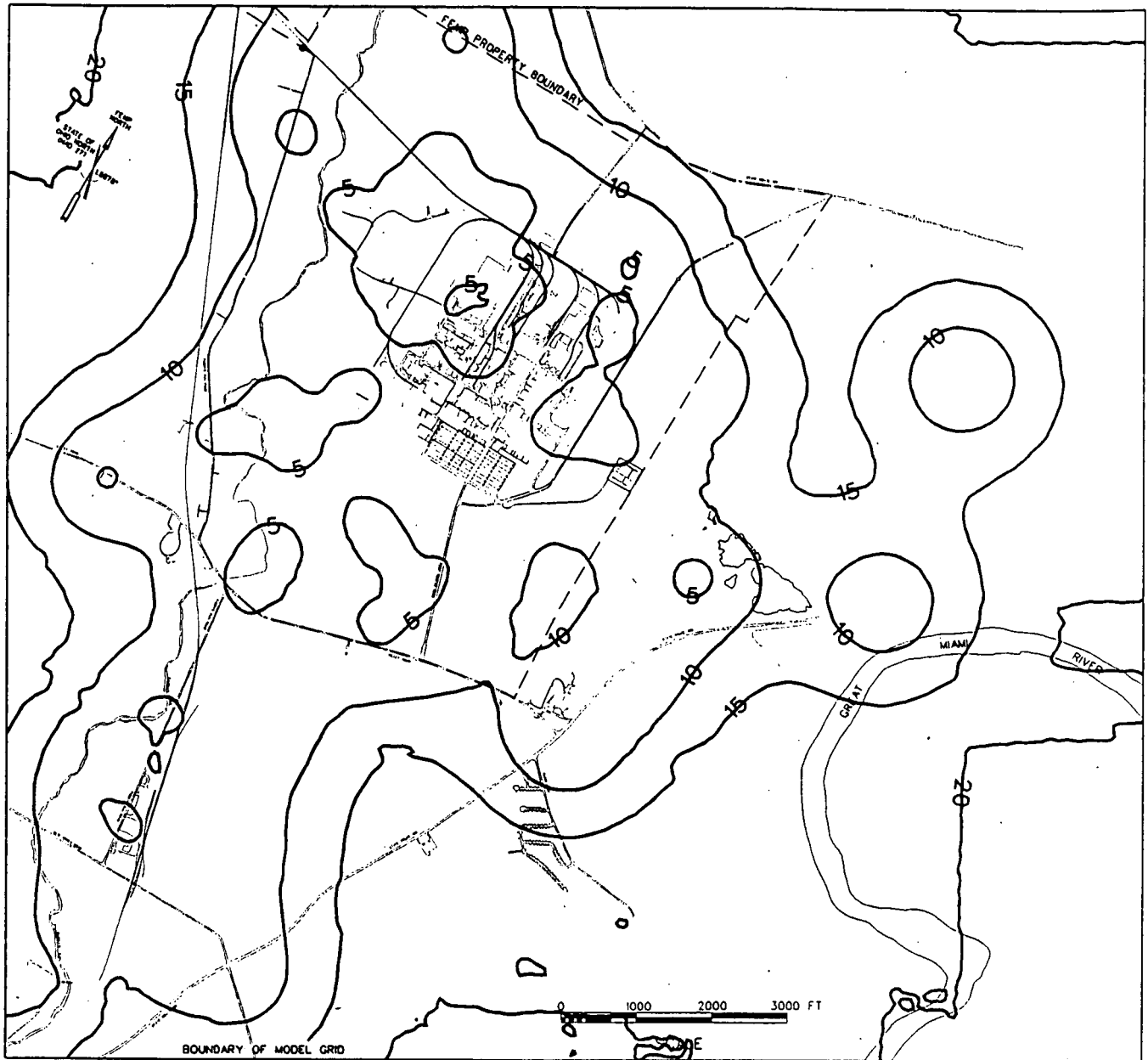


Figure 32 - Multiplicative Statistical Uncertainty Factor Associated with
1992 Uranium Concentration Estimates in 2000 Series Well Levels

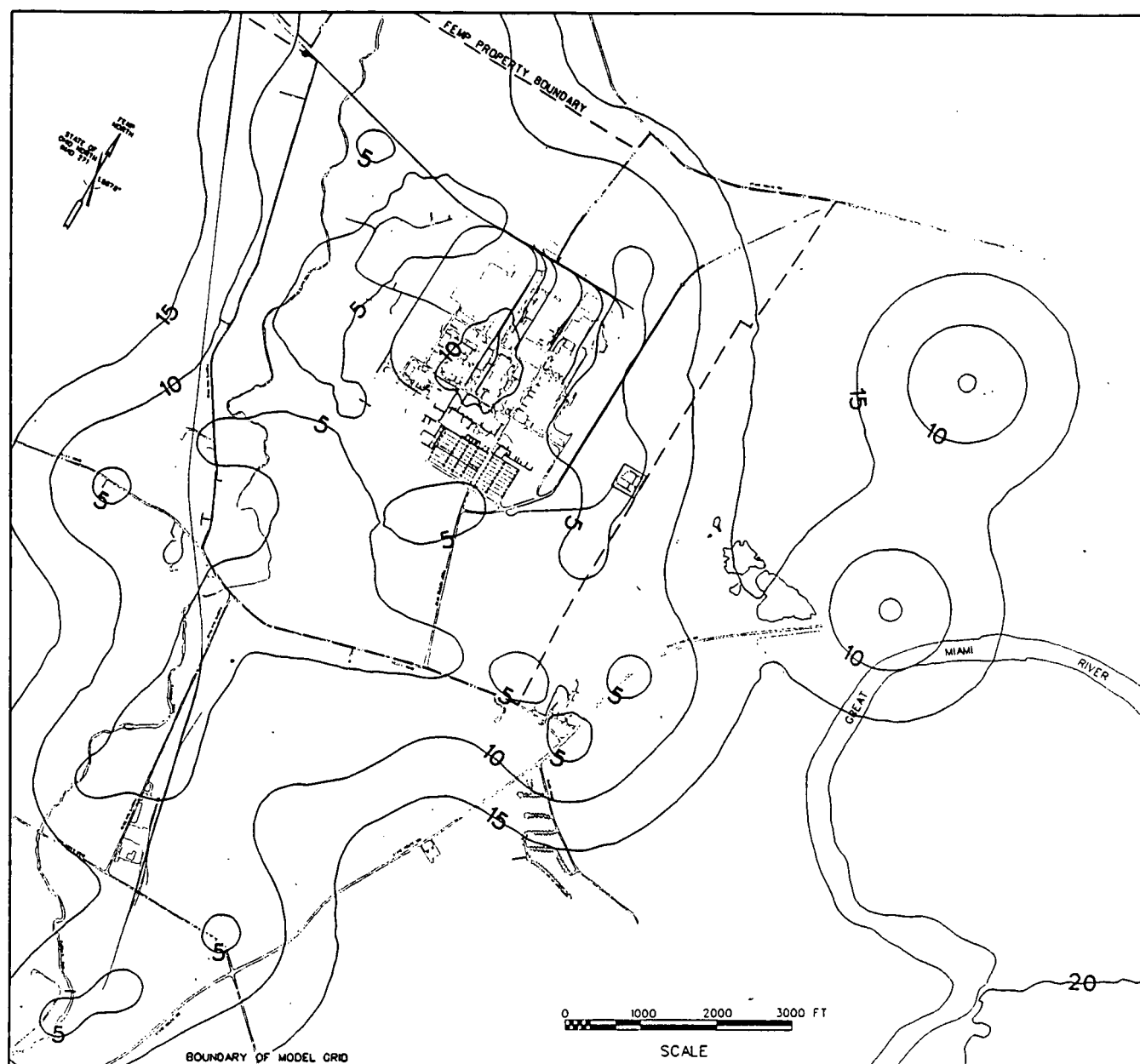


Figure 33 - Multiplicative Statistical Uncertainty Factor Associated with
1992 Uranium Concentration Estimates in 3000 Series Well Levels